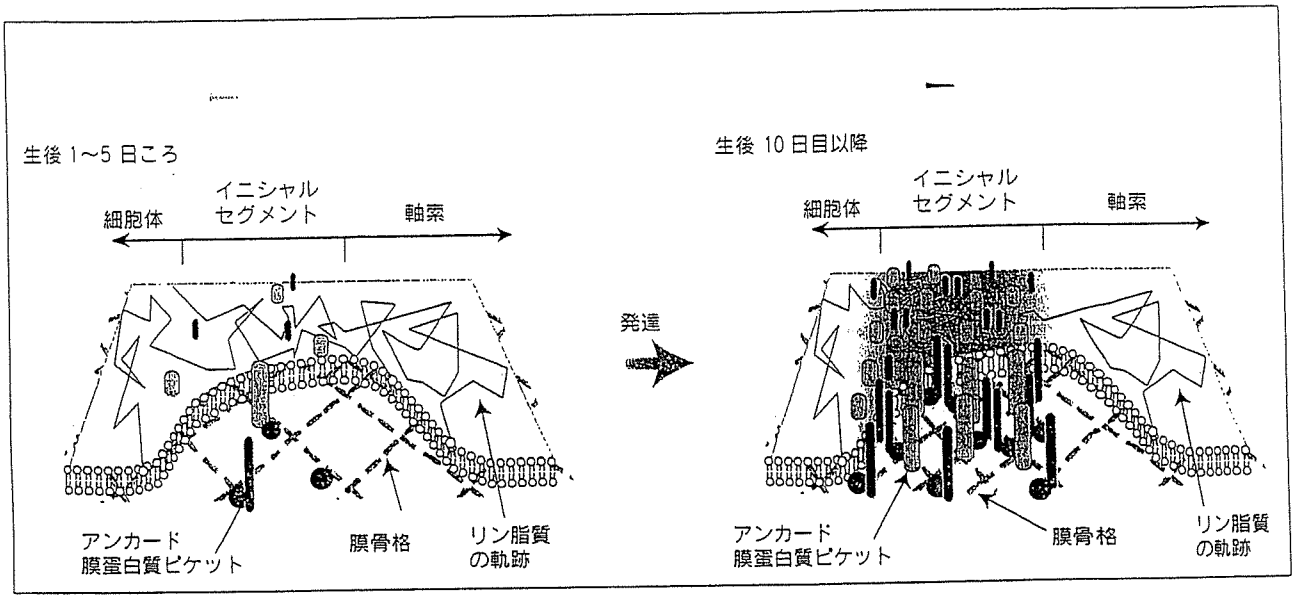

図8　拡散障壁ができる仕組み（作業仮説）

培養後間もない神経細胞のISには膜骨格や膜骨格に結合する膜蛋白質はまばらに存在しており，リン脂質の運動はそれほど制限されない．細胞の発達とともに膜骨格およびそれに結合する膜蛋白質が集積して高密度になるため，ピケット効果が大きくなり，リン脂質の拡散が大きく抑制される．このため，IS領域を通り抜けて拡散することがきわめてまれとなるので，ISの細胞膜はリン脂質の拡散に対して拡散障壁としてはたらく．

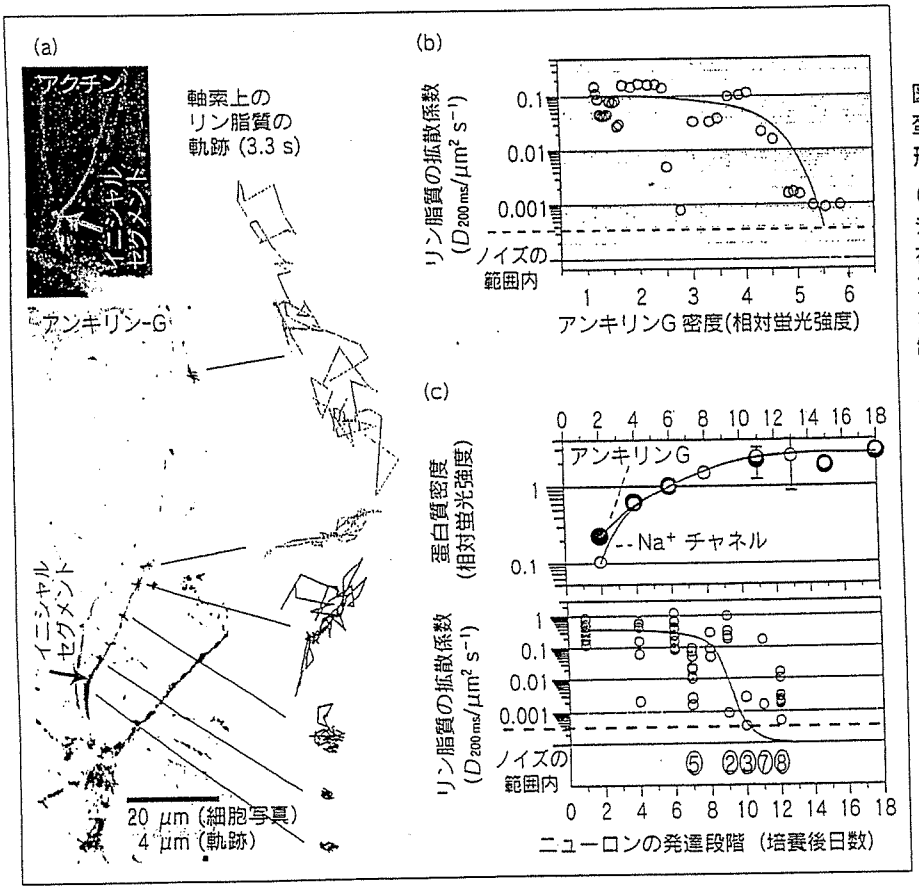

図9　拡散障壁は，膜骨格とピケット蛋白質の発達依存的な集積に伴って形成される

(a) ISにはアンキリン（写真赤）やアクチン（写真白）といった膜骨格が密に存在する．軸索上のさまざまな場所でのリン脂質の軌跡（3.3秒間）をみると，イニシャルセグメントに近づくほど拡散が抑制される．

(b) IS付近で観察したリン脂質の拡散係数を，リン脂質が運動していた微小領域のアンキリンGの密度に対してプロットしたグラフ．アンキリン密度は，リン脂質の運動を観察した後，細胞を固定し，免疫蛍光抗体法により求めた．

(c) 培養後さまざまな日数を経過した細胞のISにおけるリン脂質の拡散係数(下)と，アンキリンGおよび電位依存性Na^+チャネル（Nav1.2）のISにおける密度（上）の変化．拡散障壁は発達段階依存的に生成すること，かつ膜骨格および膜骨格結合型の膜蛋白質（ピケット蛋白質）はニューロンの発達に伴い密度が増加することがわかる．図の下の丸付き数字は，ノイズレベルに落ちてしまう拡散係数が観測されたデータの個数を示す．

に集積することによって，拡散障壁が形成されるという機構が浮かび上がってきた．

イニシャルセグメント膜にはNav1.2以外にもNrCAM, neurofascinなど，多種の膜骨格結合型の膜蛋白質の局在が知られている[36]．これらが，IS膜上のピケットラインを形成しているものと思われる．イニシャルセグメントに集積する電位依存性Na^+チャネルは活動電位の発生のために必要であるが，同時にピケット効果も発揮して拡散障壁の形成にも役立っているようである．

細胞膜上にあるマクロスコピックな拡散障壁の存在は，神経細胞以外でも数種の細胞で示唆されてきた[37,38]．しかし，境界を見る手法の制約から，あまり研究が進んでいない．今後の研究課題である．

おわりに

細胞は，膜骨格を用いて，細胞膜上の分子の拡散を制御する仕組みをもっている．これは，膜分子の会合状態の制御とともに，細胞膜分子の膜上での編制を制御するための，細胞の重要な手段の一つではないかと思われる．

このように膜骨格は，細胞が機能するために必要な細胞膜上でのいろいろなイベント（会合や信号伝達，極性維持など）を達成するうえで必須の構造である．すなわち，細胞膜がはたらく仕組みを理解するためには，“流動モザイクモデル”という従来の細胞膜の概念だけではまったく不十分であり，“膜骨格とそこに結合する膜蛋白質による仕切りが入った流動モザイク膜”という，大きなパラダイムシフトが必要である．

文　献

1) Takeuchi, M., Miyamoto, H., Sako, Y., Komizu, H., Kusumi, A. : *Biophys. J.*, 74, 2171-2183 (1998)
2) Liu, S. C., Derick, L. H., Palek, J. : *J. Cell Biol.*, 104, 527-536 (1987)
3) Picart, C., Dalhaimer, P., Discher, D. E. : *Biophys. J.*, 79, 2987-3000 (2000)
4) Shen, B. W., Josephs, R., Steck, T. L. : *J. Cell Biol.*, 102, 997-1006 (1986)
5) Fowler, V. M. : *Curr. Opin. Cell. Biol.*, 8, 86-96 (1996)
6) Grum, V. L., Li, D., MacDonald, R. I., Mondragon, A. : *Cell*, 98, 523-535 (1999)
7) McGough, A. M., Josephs, R. : *Proc. Natl. Acad. Sci. USA*, 87, 5208-5212 (1990)
8) Otto, J. J. : *Curr. Opin. Cell. Biol.*, 6, 105-109 (1994)
9) Pollard, T. D., Blanchoin, L., Mullins, R. D. : *Annu. Rev. Biophys. Biomol. Struct.*, 29, 545-576 (2000)
10) Stossel, T. P., Condeelis, J., Cooley, L., Hartwig, J. H., Noegel, A. *et al.* : *Nat. Rev. Mol. Cell Biol.*, 2, 138-145 (2001)
11) Fujiwara, T., Ritchie, K., Murakoshi, H., Jacobson, K., Kusumi, A. : *J. Cell Biol.*, 157, 1071-1081 (2002)
12) Singer, S. J., Nicolson, G. L. : *Science*, 175, 720-731 (1972)
13) Tomishige, M., Sako, Y., Kusumi, A. : *J. Cell Biol.*, 142, 989-1000 (1998)
14) Sako, Y., Nagafuchi, A., Tsukita, S., Takeichi, M., Kusumi, A. : *J. Cell Biol.*, 140, 1227-1240 (1998)
15) Sako, Y., Kusumi, A. : *J. Cell Biol.*, 129, 1559-1574 (1995)
16) Sako, Y., Kusumi, A. : *J. Cell Biol.*, 125, 1251-1264 (1994)
17) Tomishige, M., Kusumi, A. : *Mol. Biol. Cell*, 10, 2475-2479 (1999)
18) Kusumi, A., Nakada, C., Ritchie, K., Murase, K., Suzuki, K. *et al.* : *Annu. Rev. Biophys. Biomol. Struct.*, 34, 351-378 (2005)
19) Murase, K., Fujiwara, T., Umemura, Y., Suzuki, K., Iino, R. *et al.* : *Biophys. J.*, 86, 4075-4093 (2004)
20) Sperotto, M. M., Mouritsen, O. G. : *Biophys. J.*, 59, 261-270 (1991)
21) Almeida, P. F., Vaz, W. L., Thompson, T. E. : *Biochemistry*, 31, 6739-6747 (1992)
22) Bussell, S. J., Koch, D. L., Hammer, D. A. : *Biophys. J.*, 68, 1836-1849 (1995)
23) Dodd, D. S., Hammer, D. A., Sangani, A. S., Koch, D. L. : *J. Fluid Mech.*, 293, 147-180 (1995)
24) Saffman, P. G., Delbruck, M. : *Proc. Natl. Acad. Sci. USA*, 72, 3111-3113 (1975)
25) Iino, R., Koyama, I., Kusumi, A. : *Biophys. J.*, 80, 2667-2677 (2001)
26) Hegener, O., Prenner, L., Runkel, F., Baader, S. L., Kappler, J. *et al.* : *Biochemistry*, 43, 6190-6199 (2004)
27) Nelson, S., Horvat, R. D., Malvey, J., Roess, D. A., Barisas, B. G. *et al.* : *Endocrinology*, 140, 950-957 (1999)
28) Roess, D. A., Horvat, R. D., Munnelly, H., Barisas, B. G. : *Endocrinology*, 141, 4518-4523 (2000)
29) Kobayashi, T., Storrie, B., Simons, K., Dotti, C. G. : *Nature*, 359, 647-650 (1992)
30) Futerman, A. H., Khanin, R., Segel, L. A. : *Nature*, 362, 119 (1993)
31) Winckler, B., Poo, M. M. : *Nature*, 379, 213 (1996)
32) Winckler, B., Forscher, P., Mellman, I. : *Nature*, 397, 698-701 (1999)
33) Fukano, T., Hama, H., Miyawaki, A. : *J. Struct. Biol.*, 147, 12-18 (2004)
34) Nakada, C., Ritchie, K., Oba, Y., Nakamura, M., Hotta, Y. *et al.* : *Nat. Cell Biol.*, 5, 626-632 (2003)
35) Zhou, D., Lambert, S., Malen, P. L., Carpenter, S., Boland, L. M. *et al.* : *J. Cell Biol.*, 143, 1295-1304 (1998)
36) Davis, J. Q., Lambert, S., Bennett, V. : *J. Cell Biol.*, 135, 1355-1367 (1996)
37) Takizawa, P. A., DeRisi, J. L., Wilhelm, J. E., Vale, R. D. : *Science*, 290, 341-344 (2000)
38) James, P. S., Hennessy, C., Berge, T., Jones, R. : *J. Cell Sci.*, 117, 6485-6495 (2004)

Biol. Chem., Vol. 387, pp. 167–171, February 2006 • Copyright © by Walter de Gruyter • Berlin • New York. DOI 10.1515/BC.2006.022

Minireview

Anti-inflammatory effects of kinins via microglia in the central nervous system

Mami Noda[1,*], Helmut Kettenmann[2] and Keiji Wada[3]

[1] Laboratory of Pathophysiology, Graduate School of Pharmaceutical Sciences, Kyushu University, Fukuoka 812-8582, Japan
[2] Max-Delbrück Center for Molecular Medicine, D-13092 Berlin, Germany
[3] Department of Degenerative Neurological Diseases, National Institute of Neuroscience, National Center of Neurology and Psychiatry, Tokyo 187–8502, Japan

*Corresponding author
e-mail: noda@phar.kyushu-u.ac.jp

Abstract

Kinins are important biologically active peptides that are up-regulated after lesions in both the peripheral and central (CNS) nervous systems. Microglia are immune cells in the CNS and play an important role in the defense of the neuronal parenchyma. In cultured murine microglia, bradykinin (BK) induces mobilization of intracellular Ca^{2+}, microglial migration, and increases the release of nitric oxide and prostaglandin E_2. On the other hand, BK attenuates lipopolysaccharide-activated TNF-α and IL-1β release. These results suggest that BK functions as a signal in brain trauma and may have an anti-inflammatory role in the CNS.

Keywords: bradykinin; IL-1β; lipopolysaccharide; nitric oxide; prostaglandin E_2; TNF-α.

Introduction: bradykinin as a signal in brain trauma

The nonapeptide, bradykinin (BK), is an endogenous peptide produced via the kallikrein-kinin system and is widespread in the brain (Scicli et al., 1984; Chao et al., 1987; Walker et al., 1995; Raidoo and Bhoola, 1998). BK functions as a mediator of inflammation and as a vasodepressor in both the periphery and brain and is released during brain trauma such as stroke (Abbott, 2000). BK receptors are present on neurons (Walker et al., 1995; Delmas et al., 2002) and all types of glial cells, namely astrocytes and oligodendrocytes (Ritchie et al., 1987; Gimpl et al., 1992; Hosli et al., 1992; Lin and Chuang, 1992; Stephens et al., 1993a), satellite glial cells (Hanani, 2005), and microglial cells (Noda et al., 2003).

BK receptors are coupled to several intracellular signal transduction cascades (Hall, 1992; Walker et al., 1995; Noda et al., 2004a). One pathway is the mobilization of intracellular Ca^{2+} induced by inositol 1,4,5-trisphosphate (IP_3) and consequent activation of Ca^{2+}-dependent K^+ channels in NG108-15 cells (Higashida and Brown, 1988; Kim and Kim, 1998; Frieden et al., 1999). BK has been reported to induce the activation of phospholipase A_2 and stimulate arachidonic acid release (Welsh et al., 1988; Yanaga et al., 1991). BK receptors also activate $G_{i/o}$ protein (Liebmann et al., 1990; Liebmann, 2001). In astrocytes and oligodendrocytes, BK caused the release of arachidonic acid (Burch and Kniss, 1988; Kaeser et al., 1988), Ca^{2+}-dependent glutamate release (Parpura et al., 1994) and IL-6 expression (Schwaninger et al., 1999).

Microglia as a sensor of brain pathology

Following any type of brain injury, such as lesion, stroke, neurodegenerative disorders and tumor invasion, microglia are rapidly activated. Microglia are the main immune effector-cell population of the central nervous system (CNS) and control immune cell recruitment (Perry et al., 1993; Kreutzberg, 1996; Kim and de Vellis, 2005). Activated microglia migrate rapidly to the lesion site, phagocytose dead cells and clear cellular debris. As recently shown by Nimmerjahn et al. (2005) and Davalos et al. (2005), even resting microglial cells scan their environment with their processes in the intact brain.

One important question relates to the signals that initiate and promote microglial activation. Davalos et al. (2005) recently reported that adenosine trisphosphate (ATP) is an early signal controlling rapid extension of the processes towards a lesion site. Additional and subsequent signals may promote the progression and regulation of microglial activation. BK is also a candidate for such a control element.

BK induces a transient intracellular Ca^{2+} increase in microglia

In astrocytes and oligodendrocytes, BK increases phosphoinositide turnover and raises intracellular Ca^{2+} concentrations (Ritchie et al., 1987; Gimpl et al., 1992; Lin and Chuang, 1992; Stephens et al., 1993b; Bernstein et al., 1996; He et al., 1996; Simpson et al., 1997). In murine primary cultured microglia, BK receptors are also expressed and linked to IP_3 signaling, causing an intracellular Ca^{2+} rise and, as a consequence, activation of Ca^{2+}-dependent K^+ channels (Noda et al., 2003, 2004b). Only a subpopulation of 20% responded to BK, as assessed both by membrane current measurements using the patch-clamp technique and by Ca^{2+}-imaging.

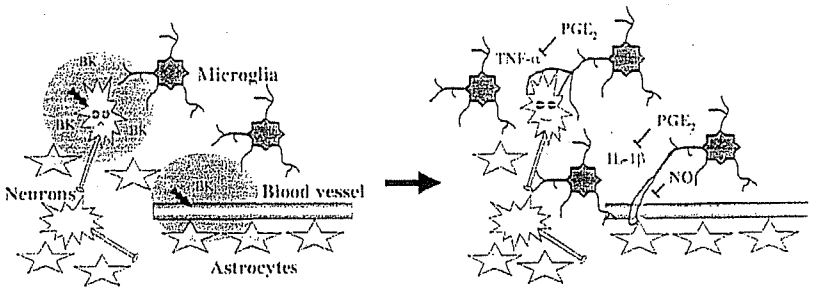

Figure 1 Proposed actions of bradykinin (BK) on microglia.
Left: in response to a pathologic event, neuropeptides, including bradykinin (BK), are released. Right: microglial cells are attracted to the lesion or inflammatory site. In response to BK, microglia release prostaglandin E_2 (PGE_2) and nitric oxide (NO). The release of inflammatory cytokines such as TNF-α and IL1-β from microglia is down-regulated by BK-induced PGE_2 as a potential neuroprotective mechanism. The impact of BK-induced microglial NO release is less evident, since it could both affect neurons and the vascular system (right).

As a reference, ATP was applied, which evoked an increase in $[Ca^{2+}]_i$ in all cells. The BK response was significantly smaller than the response to ATP. These results suggest that a minor population of cultured microglial cells express functional BK receptors.

BK increases microglial motility and induces a chemotactic response

ATP receptor activation not only stimulates the movement of processes in resting microglia, but is also a chemotactic factor for ameboid (cultured) microglial cells, which involves migration of the entire cell (Honda et al., 2001). Using time-lapse video microscopy, we have observed that BK also increased microglial motility, and that this was significantly blocked by an inhibitor of Ca^{2+}-dependent K^+ channels, charybdotoxin (Ifuku et al., 2005). Ca^{2+}-dependent K^+ channels in microglia are also important for lysophosphatidic acid (LPA)-induced migration (Schilling et al., 2004; Eder, 2005). While the BK-induced Ca^{2+} and current response rapidly desensitized, BK induced an increase in microglial motility over many hours. Since BK did not induce the increase in microglial motility in Ca^{2+}-free extracellular solution, we assume that the Ca^{2+} entry is an initial event followed by subsequent responses. As observed in thymus-derived lymphocytes (T-cells), depletion of internal Ca^{2+} stores induced by generation of IP_3 may activate voltage-independent Ca^{2+} release-activated Ca^{2+} (CRAC) channels, and chronic Ca^{2+} influx sustains elevated levels of cytosolic Ca^{2+} (Fanger et al., 2001; Chandy et al., 2004).

Although ATP increased microglial motility over a similar time course as BK, ATP-induced migration was not dependent on Ca^{2+}-dependent K^+ channels. As reported by Honda et al. (2001), ATP-induced migration was inhibited by treatment of microglial cells with pertussis toxin (PTX), suggesting that activation of $G_{i/o}$ protein induced by P2Y receptor was important. BK receptors have also been reported to couple to $G_{i/o}$ protein (Liebmann et al., 1990; Liebmann, 2001). Nevertheless, the BK-induced increase in motility was not inhibited by PTX (Ifuku et al., 2005), suggesting that BK receptors in microglia may not couple to the same $G_{i/o}$ protein, which can be activated by P2Y receptors. This indicates that ATP and BK control migration via different mechanisms, one involving activation of Ca^{2+}-dependent K^+ channels via $G_{q/11}$ signaling, and the other via $G_{i/o}$ signaling.

The motility response is mediated by B_1 receptors

BK activates two types of receptors, B_1 and B_2. The B_2 receptor is constitutively expressed in various mammalian tissues, while the B_1 receptor is expressed at very low levels under normal conditions, but is up-regulated by treatment with lipopolysaccharide (LPS) or cytokines such as interleukin-1β (IL-1β). Using specific ligands, we demonstrated that the BK-induced increase in microglial motility resulted from activation of B_1 receptors, but not B_2 receptors (Ifuku et al., 2005). This is substantiated by the finding that mRNA for the B_1 receptor was up-regulated by application of BK in rat primary cultured microglia when assessed by quantitative RT-PCR analysis (Noda et al., 2003).

BK-induced release of nitric oxide and prostaglandin E_2 from microglia

Substances involved in the process of microglial activation also control the release of various substances from microglia, including cytokines, nitric oxide (NO) and prostaglandin E_2 (PGE_2). Indeed, BK triggered the release of NO and PGE_2, but not pro-inflammatory cytokines such as tumor necrosis factor-α (TNF-α) and IL-1β, and reactive oxygen species, despite the fact that BK is considered to be a mediator of pain and inflammation. In contrast, the release of TNF-α and IL-1β induced by LPS was attenuated by BK (300–1000 nM). The attenuation of LPS-induced TNF-α and IL-1β release was likely due to the formation of PGE_2. We assume that PGE_2 acts as an autocrine factor, activating prostanoid receptors in microglia. Indeed, microglial cells express predominantly EP_2 and EP_4 receptors, which are coupled to G_s protein activation, leading to an increase in intracellular cAMP. The expression levels of the EP_2 and EP_4 receptors, as well as BK receptors (Noda et al., 2003), were up-regulated by application of BK or LPS to microglial cells. The up-

regulation of these receptors amplifies the release of PGE_2, with subsequent formation of cAMP, leading the inhibition of LPS-induced TNF-α release (Caggiano and Kraig, 1999; Webb et al., 2003). PGE_2 and cAMP were suggested to be neuroprotective (Kim et al., 2002), while COX enzymes and prostanoids are reported to mediate both neurodegeneration and neuroprotection during brain inflammation (Tzeng et al., 2005) and lack of a microglial EP_2 receptor protected against the neurotoxic effects of the cerebral innate immune response (Shie et al., 2005).

Protective effects of BK

In the CNS, microglia are the major cell population responding to LPS and this activation is mediated via a Toll-like receptor 4 (TLR4)-dependent pathway (Lehnardt et al., 2003). The BK-induced inhibition of LPS-induced TNF-α release could be protective for neurons suffering from the toxic effect of TNF-α and IL-1β. LPS-induced neuronal apoptotic cell death through the intracellular cAMP system is associated with the modulation of NO from microglial cells and reactive oxygen species (ROS) production from neurons (Kim et al., 2002). BK has anti-inflammatory effects due to its attenuation of the release of pro-inflammatory cytokines such as TNF-α and IL-1β from the microglia, and this may mediate neuroprotection. This is in contrast to the general concept of kinins as mediators of inflammatory diseases and pain, because beneficial effects of B_2 receptor antagonists have been reported (Heitsch, 2000). Furthermore, activation of neuronal B_2 receptor produces pain hypersensitivity by potentiating glutamatergic transmission (Wang et al., 2005) and induces glutamate release from astrocytes (Parpura et al., 1994). Therefore, effects of BK in microglia might be distinct from those in other cell types in the CNS.

The multiple effects of BK via microglia are summarized in Figure 1. Microglia migrate to the lesion site, react to BK, and release NO and PGE_2. In response to a lesion, BK and the expression of its receptors are up-regulated in microglia, thereby amplifying the release of PGE_2. The released PGE_2 interacts with microglial EP_2 and EP_4 receptors (which are also up-regulated by BK), increases intracellular cAMP, and down-regulates the release of TNF-α and IL-1β. The role of BK-induced NO release has not yet been elucidated, but presumably competes with the contraction of blood vessels after the lesion (Nimmerjahn et al., 2005) by amplifying the vasodilation induced by B_2 receptor-hyperpolariztion and NO-cGMP signaling (Frieden et al., 1999; Miura et al., 1999; Batenburg et al., 2005).

In conclusion, BK is a candidate important signal in brain injury. There are many neuropeptides that are elevated following neural injury and have putative roles in glia (Ubink et al., 2003). In particular, galanin has an inhibitory effect on micrgolial TNF-α production (Su et al., 2003) similar to that of BK. These results strongly indicate that BK deserves attention as a member of the family of neuropeptides, as already proposed by Hallberg and Nyberg (2003), and its protective role could be valuable for the treatment of neuropathic pain, lesion, or inflammation.

Acknowledgments

This work was supported by Grants-in-Aid for Scientific Research from the Japan Society for the Promotion of Science and from the Ministry of Health, Labor and Welfare, Japan.

References

Abbott, N.J. (2000). Inflammatory mediators and modulation of blood-brain barrier permeability. Cell Mol. Neurobiol. *20*, 131–147.

Batenburg, W.W., Tom, B., Schuijt, M.P., and Danser, A.H. (2005). Angiotensin II type 2 receptor-mediated vasodilation. Focus on bradykinin, NO and endothelium-derived hyperpolarizing factor(s). Vascul. Pharmacol. *42*, 109–118.

Bernstein, M., Lyons, S.A., Moller, T., and Kettenmann, H. (1996). Receptor-mediated calcium signalling in glial cells from mouse corpus callosum slices. J. Neurosci. Res. *46*, 152–163.

Burch, R.M. and Kniss, D.A. (1988). Modulation of receptor-mediated signal transduction by diacylglycerol mimetics in astrocytes. Cell Mol. Neurobiol. *8*, 251–257.

Caggiano, A.O. and Kraig, R.P. (1999). Prostaglandin E receptor subtypes in cultured rat microglia and their role in reducing lipopolysaccharide-induced interleukin-1β production. J. Neurochem. *72*, 565–575.

Chandy, K.G., Wulff, H., Beeton, C., Pennington, M., Gutman, G., and Cahalan, M.D. (2004). K^+ channels as targets for specific immunomodulation. Trends. Pharmacol. Sci. *25*, 280–289.

Chao, J., Chao, L., Swain, C.C., Tsai, J., and Margolius, H.S. (1987). Tissue kallikrein in rat brain and pituitary: regional distribution and estrogen induction in the anterior pituitary. Endocrinology *120*, 475–482.

Davalos, D., Grutzendler, J., Yang, G., Kim, J.V., Zuo, Y., Jung, S., Littman, D.R., Dustin, M.L., and Gan, W.B. (2005). ATP mediates rapid microglial response to local brain injury *in vivo*. Nat. Neurosci. *8*, 752–758.

Delmas, P., Wanaverbecq, N., Abogadie, F.C., Mistry, M., and Brown, D.A. (2002). Signaling microdomains define the specificity of receptor-mediated $InsP_3$ pathways in neurons. Neuron *14*, 209–220.

Eder, C. (2005). Regulation of microglial behavior by ion channel activity. J. Neurosci. Res. *81*, 314–321.

Fanger, C.M., Rauer, H., Neben, A.L., Miller, M.J., Rauer, H., Wulff, H., Rosa, J.C., Ganellin, C.R., Chandy, K.G., and Cahalan, M.D. (2001). Calcium-activated potassium channels sustain calcium signaling in T lymphocytes. Selective blockers and manipulated channel expression levels. J. Biol. Chem. *276*, 12249–12256.

Frieden, M., Sollini, M., and Beny, J. (1999). Substance P and bradykinin activate different types of KCa currents to hyperpolarize cultured porcine coronary artery endothelial cells. J. Physiol. *519*, 361–371.

Gimpl, G., Walz, W., Ohlemeyer, C., and Kettenmann, H. (1992). Bradykinin receptors in cultured astrocytes from neonatal rat brain are linked to physiological responses. Neurosci. Lett. *144*, 139–142.

Hall, J.M. (1992). Bradykinin receptors: pharmacological properties and biological roles. Pharmacol. Ther. *56*, 131–190.

Hallberg, M. and Nyberg, F. (2003). Neuropeptide conversion to bioactive fragments – an important pathway in neuromodulation. Curr. Protein Pept. Sci. *4*, 31–44.

Hanani, M. (2005). Satellite glial cells in sensory ganglia: from form to function. Brain Res. Brain Res. Rev. *48*, 457–476.

He, M., Howe, D.G., and McCarthy, K.D. (1996). Oligodendroglial signal transduction systems are regulated by neuronal contact. J. Neurochem. *67*, 1491–1499.

Heitsch, H. (2000). Bradykinin B2 receptor as a potential therapeutic target. Drug News Perspect. *13*, 213–225.

Higashida, H. and Brown, D.A. (1988). Ca^{2+}-dependent K^+ channels in neuroblastoma hybrid cells activated by intracellular inositol trisphosphate and extracellular bradykinin. FEBS Lett. *238*, 395–400.

Honda, S., Sasaki, Y., Ohsawa, K., Imai, Y., Nakamura, Y., Inoue, K., and Kohsaka, S. (2001). Extracellular ATP or ADP induce chemotaxis of cultured microglia through $G_{i/o}$-coupled P2Y receptors. J. Neurosci. *21*, 1975–1982.

Hosli, L., Hosli, E., Kaeser, H., and Lefkovits, M. (1992). Colocalization of receptors for vasoactive peptides on astrocytes of cultured rat spinal cord and brain stem: electrophysiological effects of atrial and brain natriuretic peptide, neuropeptide Y and bradykinin. Neurosci. Lett. *148*, 114–116.

Ifuku, M., Wang, B., and Noda, M. (2005). Activation of Ca^{2+}-dependent K^+ channels is essential for bradykinin-induced microglial migration. In: VII European Meeting on Glial Cell Function in Health and Disease, 19–25 May 2005, Amsterdam, Netherlands (Bologna, Italy: Medimond S.r.l.), pp. 97–101.

Kaeser, F., Luthy, C., Herschkowitz, N., and Oetliker, O. (1988). The effect of temporary hypoxia on prostaglandin synthesis in mouse brain cell cultures during development. Prostaglandins Leukot. Essent. Fatty Acids *32*, 75–81.

Kim, E.J., Kwon, K.J., Park, J.Y., Lee, S.H., Moon, C.H., and Baik, E.J. (2002). Neuroprotective effects of prostaglandin E_2 or cAMP against microglial and neuronal free radical mediated toxicity associated with inflammation. J. Neurosci. Res. *70*, 97–107.

Kim, S.J. and Kim, J. (1998). Relation of exocytosis and Ca^{2+}-activated K^+ current during Ca^{2+} release from intracellular stores in individual rat chromaffin cells. Brain Res. *799*, 197–206.

Kim, S.U. and de Vellis, J. (2005). Microglia in health and disease. J. Neurosci. Res. *81*, 302–313.

Kreutzberg, G.W. (1996). Microglia: a sensor for pathological events in the CNS. Trends Neurosci. *19*, 312–318.

Lehnardt, S., Massillon, L., Follett, P., Jensen, F.E., Ratan, R., Rosenberg, P.A., Volpe, J.J., and Vartanian, T. (2003). Activation of innate immunity in the CNS triggers neurodegeneration through a Toll-like receptor 4-dependent pathway. Proc. Natl. Acad. Sci. USA *100*, 8514–8519.

Liebmann, C. (2001). Bradykinin signalling to MAP kinase: cell-specific connections versus principle mitogenic pathways. Biol. Chem. *382*, 49–55.

Liebmann, C., Offermanns, S., Spicher, K., Hinsch, K.D., Schnittler, M., Morgat, J.L., Reissmann, S., Schultz, G., and Rosenthal, W. (1990). A high-affinity bradykinin receptor in membranes from rat myometrium is coupled to pertussis toxin-sensitive G proteins of the G_i family. Biochem. Biophys. Res. Commun. *167*, 910–917.

Lin, W.W. and Chuang, D.M. (1992). Regulation of bradykinin-induced phosphoinositide turnover in cultured cerebellar astrocytes: possible role of protein kinase C. Neurochem. Int. *21*, 573–579.

Miura, H., Liu, Y., and Gutterman, D.D. (1999). Human coronary arteriolar dilation to bradykinin depends on membrane hyperpolarization: contribution of nitric oxide and Ca^{2+}-activated K^+ channels. Circulation *99*, 3132–3138.

Nimmerjahn, A., Kirchhoff, F., and Helmchen, F.R. (2005). Resting microglial cells are highly dynamic surveillants of brain parenchyma *in vivo*. Science *308*, 1314–1318.

Noda, M., Kariura, Y., Amano, T., Manago, Y., Nishikawa, K., Aoki, S., and Wada, K. (2003). Expression and function of bradykinin receptors in microglia. Life Sci. *72*, 1573–1581.

Noda, M., Kariura, Y., Amano, T., Manago, Y., Nishikawa, K., Aoki, S., and Wada, K. (2004a). Kinin receptors in cultured rat microglia. Neurochem. Int. *45*, 437–442.

Noda, M., Kariura, Y., Kosai, Y., Pannasch, U., Wang, L., Kettenmann, H., Nishikawa, K., Okada, S., Aoki, S., and Wada, K. (2004b). Inflammation in the CNS: the role of bradykinin in glial cells. J. Neurochem. *88* (Suppl. 1), 11.

Parpura, V., Basarsky, T.A., Liu, F., Jeftinija, K., Jeftinija, S., and Haydon, P.G. (1994). Glutamate-mediated astrocyte-neuron signalling. Nature *369*, 744–747.

Perry, V.H., Andersson, P.B., and Gordon, S. (1993). Macrophages and inflammation in the central nervous system. Trends Neurosci. *16*, 268–273.

Raidoo, D.M. and Bhoola, K.D. (1998). Pathophysiology of the kallikrein-kinin system in mammalian nervous tissue. Pharmacol. Ther. *79*, 105–127.

Ritchie, T., Cole, R., Kim, H.S., de Vellis, J., and Noble, E.P. (1987). Inositol phospholipid hydrolysis in cultured astrocytes and oligodendrocytes. Life Sci. *41*, 31–39.

Schilling, T., Stock, C., Schwab, A., and Eder, C. (2004). Functional importance of Ca^{2+}-activated K^+ channels for lysophosphatidic acid-induced microglial migration. Eur. J. Neurosci. *19*, 1469–1474.

Schwaninger, M., Sallmann, S., Petersen, N., Schneider, A., Prinz, S., Libermann, T.A., and Spranger, M. (1999). Bradykinin induces interleukin-6 expression in astrocytes through activation of nuclear factor-κB. J. Neurochem. *73*, 1461–1466.

Scicli, A.G., Forbes, G., Nolly, H., Dujovny, M., and Carretero, O.A. (1984). Kallikrein-kinins in the central nervous system. Clin. Exp. Hypertens. A *6*, 1731–1738.

Shie, F.S., Montine, K.S., Breyer, R.M., and Montine, T.J. (2005). Microglial EP2 as a new target to increase amyloid beta phagocytosis and decrease amyloid β-induced damage to neurons. Brain Pathol. *15*, 134–138.

Simpson, P.B., Mehotra, S., Lange, G.D., and Russell, J.T. (1997). High density distribution of endoplasmic reticulum proteins and mitochondria at specialized Ca^{2+} release sites in oligodendrocyte processes. J. Biol. Chem. *272*, 22654–22661.

Stephens, G.J., Marriott, D.R., Djamgoz, M.B., and Wilkin, G.P. (1993a). Electrophysiological and biochemical evidence for bradykinin receptors on cultured rat cortical oligodendrocytes. Neurosci. Lett. *153*, 223–226.

Stephens, G.J., Cholewinski, A.J., Wilkin, G.P., and Djamgoz, M.B. (1993b). Calcium-mobilizing and electrophysiological effects of bradykinin on cortical astrocyte subtypes in culture. Glia *9*, 269–279.

Su, Y., Ganea, D., Peng, X., and Jonakait, G.M. (2003). Galanin down-regulates microglial tumor necrosis factor-α production by a post-transcriptional mechanism. J. Neuroimmunol. *134*, 52–60.

Tzeng, S.F., Hsiao, H.Y., and Mak, O.T. (2005). Prostaglandins and cyclooxygenases in glial cells during brain inflammation. Curr. Drug Targets Inflamm. Allergy *4*, 335–340.

Ubink, R., Calza, L., and Hokfelt, T. (2003). 'Neuro'-peptides in glia: focus on NPY and galanin. Trends Neurosci. *26*, 604–609.

Walker, K., Perkins, M., and Dray, A. (1995). Kinins and kinin receptors in the nervous system. Neurochem. Int. *26*, 1–16.

Wang, H., Kohno, T., Amaya, F., Brenner, G.J., Ito, N., Allchorne, A., Ji, R.R., and Woolf, C.J. (2005). Bradykinin produces pain hypersensitivity by potentiating spinal cord glutamatergic synaptic transmission. J. Neurosci. *25*, 7986–7992.

Webb, J.G., Shearer, T.W., Yates, P.W., Mukhin, Y.V., and Crosson, C.E. (2003). Bradykinin enhancement of PGE_2 signalling in bovine trabecular meshwork cells. Exp. Eye. Res. *76*, 283–289.

Welsh, C., Dubyak, G., and Douglas, J.G. (1988). Relationship

between phospholipase C activation and prostaglandin E_2 and cyclic adenosine monophosphate production in rabbit tubular epithelial cells. Effects of angiotensin, bradykinin, and arginine vasopressin. J. Clin. Invest. *81*, 710–719.

Yanaga, F., Hirata, M., and Koga, T. (1991). Evidence for coupling of bradykinin receptors to a guanine-nucleotide binding protein to stimulate arachidonate liberation in the osteoblast-like cell line, MC3T3-E1. Biochim. Biophys. Acta *1094*, 139–146.

Available online at www.sciencedirect.com
SCIENCE DIRECT
ELSEVIER
Biochemical and Biophysical Research Communications 342 (2006) 867–874
BBRC
www.elsevier.com/locate/ybbrc

TrkB-T1 regulates the RhoA signaling and actin cytoskeleton in glioma cells

Koji Ohira [a,b], Koichi J. Homma [c], Hirohisa Hirai [a], Shun Nakamura [b], Motoharu Hayashi [a,*]

[a] *Department of Cellular and Molecular Biology, Primate Research Institute, Kyoto University, Aichi, Japan*
[b] *Department of Biochemistry and Cellular Biology, National Institute of Neuroscience, National Center of Neurology and Psychiatry, Tokyo, Japan*
[c] *Department of Molecular Pathology, Faculty of Pharmaceutical Sciences, Teikyo University, Kanagawa, Japan*

Received 30 January 2006
Available online 20 February 2006

Abstract

Recently, the truncated TrkB receptor, T1, has been reported to be involved in the control of cell morphology via the regulation of Rho proteins, through which T1 binds Rho guanine nucleotide dissociation inhibitor (Rho GDI) 1 and dissociates it in a brain-derived neurotrophic factor (BDNF)-dependent manner. However, it is unclear whether T1 signaling regulates the downstream of Rho signaling and the actin cytoskeleton. In this study, we investigated this question using C6 rat glioma cells, which express T1 endogenously. Rho GDI1 was dissociated from T1 in a BDNF-dependent manner, which also causes decreases in the activities of Rho-signaling molecules such as RhoA, Rho-associated kinase, p21-activated kinase, and extracellular-signal regulated kinase1/2. Moreover, BDNF treatment resulted in the disappearance of stress fibers in the cells treated with lysophosphatidic acid, an activator of RhoA, and in morphological changes in cells. Furthermore, a competitive assay with cyan fluorescent protein fusion proteins of T1-specific sequences reduced the effects of BDNF. These results suggest that T1 regulates the Rho-signaling pathways and the actin cytoskeleton.

Keywords: BDNF; Cell morphology; ERK; In vitro; Neurotrophin; PAK; ROCK; Signal transduction; TrkB receptor

Neurotrophins belong to the nerve growth factor (NGF) family and in mammals consist of NGF, brain-derived neurotrophic factor (BDNF), NT-3, and NT-4. Their receptors are the tropomyosin related kinase (Trk) receptor family. TrkA recognizes NGF, both BDNF and NT-4 are ligands for TrkB, and TrkC is an NT-3 receptor [1].

In the mammalian central nervous system (CNS), BDNF, and TrkB are enriched [2–4] and function as survival, differentiation, morphogenic, and growth factors during early development, and as mediators of neural plasticity in the adult stage [5,6]. The TrkB gene encodes at least three subtypes: TK+, T1, and T2 [1]. TK+ has its signaling pathways via tyrosine kinases such as Ras, phosphatidylinositide 3-kinase, and phospholipase C-γ [7]. In contrast, T1 and T2 possess specific 11- and 9-amino acid sequences, respectively, in the C-terminal instead of tyrosine kinases. The T1-specific amino acid sequence is completely conserved from mice to humans [8–10]. Furthermore, the TrkB subtypes show characteristic expression patterns during the development of the mammalian CNS [4,11,12]. TK+ is detected at the same levels from embryonic to adult periods, while the expression of T1 increases remarkably during the late developmental period and is maintained to adulthood. Moreover, in the prefrontal cortex of the adult monkey, TK+ homodimer cannot be detected, but T1 homodimer and TK+–T1 heterodimer are formed in a BDNF-dependent manner [13]. Thus, these findings suggest that T1 plays an important role in such functions as neural plasticity and maintenance during the adult period.

Recently, T1 has been reported to regulate the morphology of both neurons [14,15] and glias [16,17] as well as calcium entry into astrocytes [18]. For example, the

* Corresponding author. Fax: +81 568 63 0085.
E-mail address: hayashi@pri.kyoto-u.ac.jp (M. Hayashi).

0006-291X/$ - see front matter © 2006 Elsevier Inc. All rights reserved.
doi:10.1016/j.bbrc.2006.02.033

overexpression of T1 induces the elongation of and an increase in the branch number of distal dendrites of cortical pyramidal neurons in slices [14]. In hippocampal cultures, T1 expression has been found to increase the number of dendritic filopodia [15]. Both reports point out that the T1-induced elongation of dendrites and filopodia occurs independently of ligand binding. Therefore, it is of great interest to elucidate the T1 signaling mechanism; nevertheless, this mechanism remains unclear to date, a decade after the discovery of T1. Most recently, T1 has been reported to regulate cell morphology via Rho guanine nucleotide dissociation inhibitor (Rho GDI) 1 in primary astrocytic cultures [16]. Rho GDI1 is a negative regulator of Rho GTPases [19], which may explain in part the previous data that T1 regulates neuronal morphology [14,15]. However, it remains unclear whether T1 regulates the downstream effectors of its signaling pathway and the actin cytoskeleton. In the present study, we elucidate the missing link between Rho GDI1 and cell morphology.

Materials and methods

Cell culture. C6 cells (Dainippon Pharmaceutical, Osaka, Japan) were maintained in Ham's F-10 (Gibco, Rockville, MD, USA) supplemented with 15% horse serum (Gibco) and 2.5% fetal bovine serum (Gibco) in a humidified atmosphere containing 5% CO_2 at 37 °C. In this experiment, cells were cultured to subconfluency (70–80%) in 10-cm dishes in serum-free Ham's F-10 containing N2 supplement (Gibco) for 24 h. For administration of reagents, cells were stimulated for 30 min at 37 °C with 20 ng/ml BDNF (PeproTech, Rocky Hill, NJ, USA), anti-BDNF antibody (5 μg/ml, Santa Cruz Biotechnology, Santa Cruz, CA, USA), anti-p75 antibody (clone MC192, 1/50 of culture medium), or 10 μM LPA (Sigma, St. Louis, MO, USA). Cells were also incubated with one reagent for 30 min and subsequently incubated with another for 30 min.

Reverse transcription-polymerase chain reaction (RT-PCR). Total RNA was isolated from the cortex of adult Wistar rats (2 males, 3 months old) or C6 cells using ISOGEN (Nippon Gene, Tokyo, Japan). Reverse transcription was performed with superscript-II (Gibco) and the cDNA was amplified by PCR with primers specific for TK+ (603 bp), 5′-TCAGCAACGACGATGACTCT-3′ and 5′-AGTGTTGGGATGC CAGGTAG-3′; T1 (615 bp), 5′-CCTCGTCGGAGAAGATCAAG-3′ and 5′-TCCAGGGGGATCTTATGAAA-3′; T2 (598 bp), 5′-CAGA AAACCTCGTCGGAGAA-3′ and 5′-TGCTTACCTTTCATGCCAAA-3′; and actin (349 bp), 5′-TAAAACGCAGCTCAGTAACAGTCCG-3′ and 5′-TGGAATCCTGTGGCATCCATGAAAC-3′. The PCR was carried out as follows: DNA was denatured for 2 min at 94 °C and sequences were amplified for 30 cycles (94 °C for 30 s; 58 °C for 30 s; 72 °C for 60 s). The PCR products were separated on 2% agarose gel.

DNA constructs and transfection. We used the DNA constructs created in our previous study [16]. Briefly, vectors of enhanced cyan fluorescent protein (ECFP)-Δ11 and ECFP-1CD were prepared by PCR, using the 5′ primer, GGTCTGCCGTCTGCACGTCTG, and the 3′ primers Δ11, CGCGGATCCTTAACCTTTCATGCC; and 1CD, CGCGGATCC CCCAGCCTTGTCTTTCCTTTATC. Underlining indicates *Bam*HI sites, and boldface letters represent mutation sites. The PCR products were first digested by *Bam*HI and were then subcloned into pECFP-C1 (Clontech, Palo Alto, CA, USA). These constructs were transfected into C6 cells (50% confluent) with FuGENE6 (Roche, Basel, Switzerland).

Precipitation assays. Cells plated in a 10-cm dish were lysed with 200 μl of lysis buffer (for co-immunoprecipitation of TrkB, 10 mM triethanolamine, 10 mM iodoacetamine, pH 7.8, 150 mM NaCl, 2 mM EDTA, 1% digitonin, 1 mM phenylmethylsulfonyl fluoride (PMSF), 10 μg/ml leupeptin, and 20 μg/ml aprotinin; for precipitation of RhoA, phosphorylated PAK, phosphorylated Rho-associated kinase (ROCK), 50 mM Tris–HCl, pH 7.5, 150 mM NaCl, 5 mM MgCl2, 0.5% Triton X-100, 1 mM PMSF, 10 μg/ml leupeptin, 20 μg/ml aprotinin, and 10 nM microcystin LR). The lysates were centrifuged at 10,000*g* at 4 °C for 20 min, and the protein contents of the supernatants were determined and adjusted at 1 mg total protein/ml.

For the precipitation of TrkB, PAK, and ROCK, after incubation with preimmune IgG-protein A or G (Amersham Pharmacia Biotechnology, Tokyo, Japan) at 4 °C for 1 h, the supernatants were incubated with the indicated antibodies at 4 °C for 1 h and then with 20 μl of protein A or G Sepharose at 4 °C for 1 h. The complexes were washed once with lysis buffer containing 300 mM NaCl and 3× with lysis buffer. They were then mixed with 40 μl sodium dodecyl sulfate (SDS) sample buffer and boiled for 3 min.

For the RhoA pull-down assay, we used Rhotekin beads (Upstate Biotechnology, Charlottesville, VA, USA) following the method described by Ren et al. [20]. Briefly, the Rhotekin beads (30 μl) were added to the lysates (500 μg protein/ml) and incubated at 4 °C for 45 min. The beads were then washed 3× with lysis buffer. The resultant pellets were mixed with 40 μl SDS sample buffer and boiled for 3 min.

Western blot analysis. Samples (5 μg/lane for Rho GDI1, RhoA, ERK1/2, PAK, and ROCK; 150 μg/lane for TrkB; 20 μl for precipitation) were subjected to SDS–polyacrylamide gel electrophoresis (PAGE) (7% gel for TrkB and ROCK, 10% gel for extracellular-signal regulated kinase (ERK) 1/2 and PAK, and 12% gel for Rho GDI1 and RhoA) and blotted onto polyvinylidene difluoride (PVDF) membranes (Millipore, Billerica, MA, USA). The membranes were blocked in 5% skim milk in phosphate-buffered saline (PBS). After incubation with the indicated antibodies at room temperature for 1 h, blots were incubated with the secondary antibodies conjugated with horseradish peroxidase (HRP) and visualized by the enhanced chemiluminescence (ECL) system (Amersham Pharmacia Biotechnology).

Immunocytochemistry. Cells were grown on 12-mm diameter plastic sheets at 1000 cells/30 mm dish. The cells were fixed for 20 min in 3.7% formaldehyde in PBS and permeabilized for 20 min in PBS containing 0.1% Triton X-100. To retrieve the antigenicity of T1, the samples were preincubated in 6 M guanidine chloride in 50 mM Tris–HCl, pH 10.2, at room temperature for 15 min [16,17,21,22]. The samples were incubated at room temperature for 1 h with anti-TK+ antibody (diluted at 1/1600; Santa Cruz Biotechnology), anti-T1 antibody (diluted at 1/1600; Santa Cruz Biotechnology), or vehicle as control (PBS containing 4% normal goat serum and 1% bovine serum albumin (BSA)). They were incubated with a biotinylated secondary antibody at room temperature for 1 h. The immunoreactive sites were visualized by the avidin–biotin complex peroxidase method using an ABC elite kit (Vector Laboratories, Burlingame, CA, USA). A solution of 0.3% H_2O_2, 20 μg/ml 3,3′-diaminobenzidine tetrahydrochloride, and 0.3% nickel ammonium sulfate in 0.05 M Tris–HCl buffer, pH 7.6, was used as the substrate of the peroxidase. The plastic sheets were mounted on glass slides with Permafluor (Thermo Shandon, Pittsburgh, PA, USA).

Morphology assay. Fixed cells were incubated with 0.1 μg/ml fluorescein isothiocyanate (FITC)-phalloidin (Molecular Probes, Eugene, OR, USA) at room temperature for 20 min. The cells were counterstained with propidium iodide to visualize nuclei [23]. The samples were analyzed using a phase contrast microscope and a Zeiss confocal microscope (LSM 510; Carl Zeiss Japan, Tokyo, Japan). Three different morphologies were distinguished: (1) fully round, or round shape with extensions shorter than the soma diameter; (2) spindle or round shape with extensions longer than the soma diameter; (3) flat shape with thinly stretched extensions.

Results

Expression of T1 in C6 cells

Neurons have been found to contain both TK+ and T1 [16,17,21,22,24], while glial cells express primarily T1 [16,24]. Thus, we made use of C6 cells derived from rat

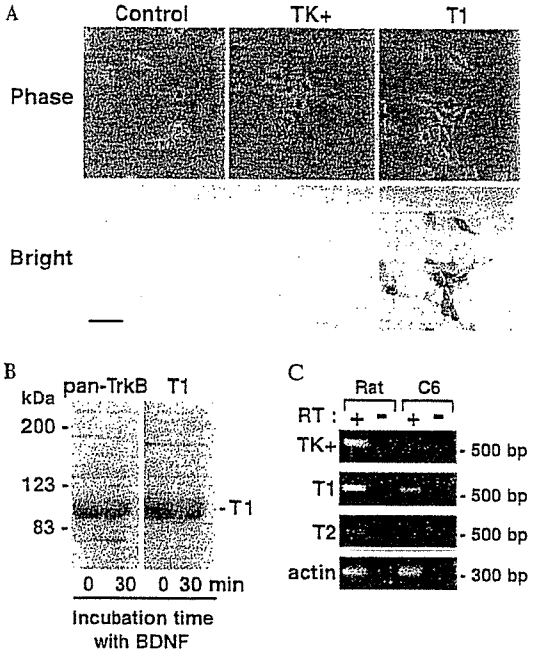

Fig. 1. Expression of the truncated TrkB receptor, T1, in C6 cells. (A) Immunocytochemistry of TK+ and T1 in C6 cells. Scale bar, 30 μm. (B) Western blot analysis of T1 in C6 cells, using anti-pan-TrkB and anti-T1 antibodies, at 0 and 30 min after stimulation with BDNF (20 ng/ml). (C) RT-PCR analysis of TrkB expression in the cerebral cortex of adult rats (3 months old) and C6 cells. BDNF, brain-derived neurotrophic factor; RT, reverse transcription.

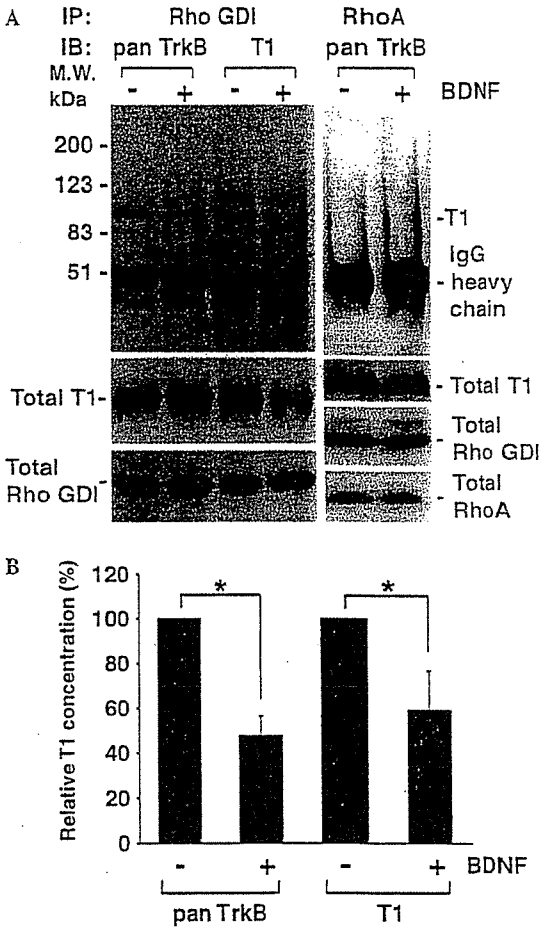

Fig. 2. Dissociation of Rho GDI1 from T1 by BDNF. (A) Co-immunoprecipitation of T1 with anti-Rho GDI1 (left column) or anti-RhoA (right column) after BDNF stimulation (20 ng/ml). T1 was detected with anti-pan-TrkB or T1 antibody. IP, immunoprecipitation; IB, immunoblot; M.W., molecular weight. (B) Quantitative analysis of the bands in (A). Control levels were taken as 100%. The asterisks indicate statistically significant differences ($p < 0.05$ by paired Student's t test). Values are given as means ± SD from four independent experiments.

glioma cells to investigate the signaling mechanism of T1; detected T1, but not TK+, in these cells (Fig. 1). We further confirmed by RT-PCR analysis that only T1 mRNA is expressed in C6 cells (Fig. 1C), and that the BDNF treatment did not induce TK+ within 30 min (Fig. 1B). Furthermore, we did not detect any expression of Rac or Cdc42 at the protein level by Western blot analysis (data not shown), which is consistent with previous results [25]. Thus, we focused primarily on analyzing the RhoA-signaling mechanism in C6 cells.

BDNF-induced dissociation of Rho GDI1 from T1

Using C6 cells, we examined whether BDNF stimulation dissociated Rho GDI1 from T1 in a BDNF-dependent manner. After BDNF stimulation (final concentration, 20 ng/ml), the T1 band was reduced to ≈50% of the control value (Fig. 2), suggesting that treatment with BDNF causes Rho GDI1 to dissociate from T1; this result is consistent with our previous results [16]. In addition, RhoA was not directly bound to T1 (right column in Fig. 2A).

Control of Rho-signaling pathways

Rho GDI1 has been shown to interact with guanosine diphosphate (GDP)-bound forms of Rho guanosine triphosphatases (GTPases) and to inhibit their conversion from GDP-bound inactive forms to guanosine triphosphate (GTP)-bound active forms [19]. Next, we investigated the effect of T1-Rho GDI1 on RhoA activated by LPA and performed a pull-down assay of the active form of RhoA. LPA treatment (10 μM) was found to increase the activity of RhoA up to 170% of the control value (Fig. 3A). Moreover, the RhoA activation triggered by LPA was reduced to the control level by BDNF treatment (20 ng/ml).

Among the numerous effector molecules of RhoA, ROCK is interesting since it is involved in various cellular functions, such as the control of smooth muscle contraction and stress fiber formation. This effect is mediated by the phosphorylation of the myosin light chain and LIM (LIM is an acronym of the three gene products Lin-11, Isl-1, and Mec-3) kinase, and the inactivation of myosin phosphatase [19,26,27]. Next, we examined whether ROCK is involved in T1 signaling. ROCK phosphorylation was found to increase significantly to 138% of the control level

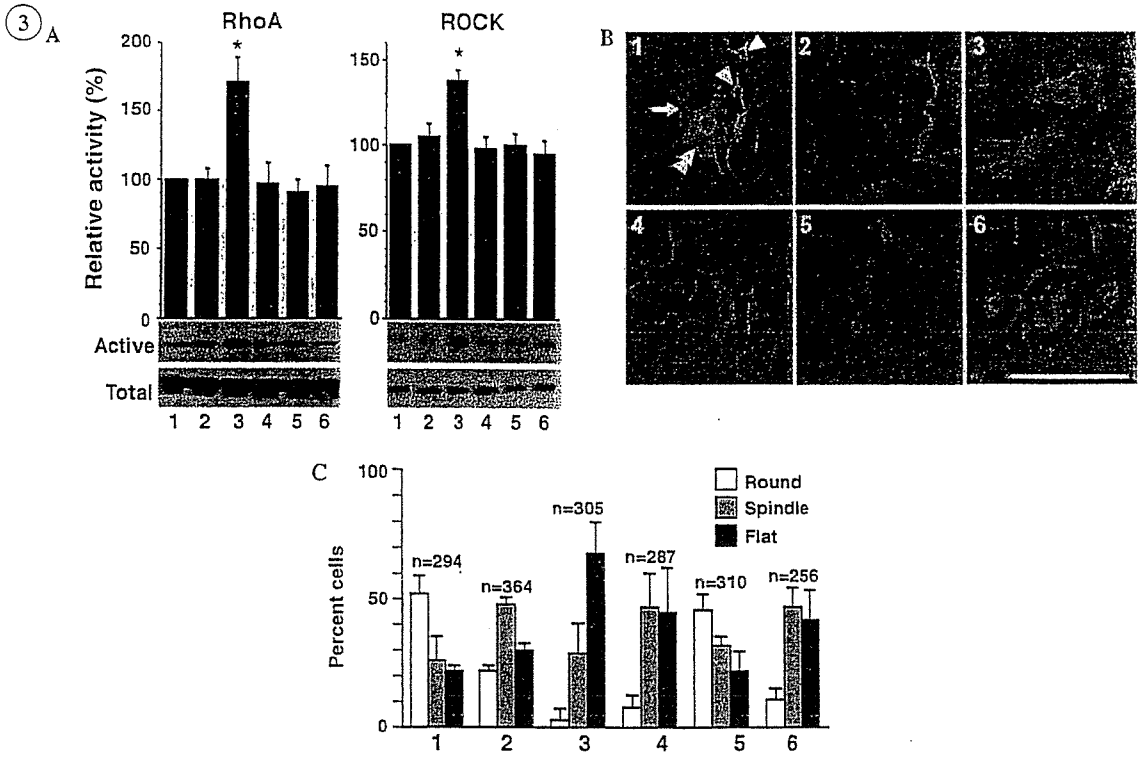
3
A
RhoA
ROCK
Relative activity (%)
200
150
100
50
0
Active
Total
1 2 3 4 5 6
B
1
2
3
4
5
6
C
Percent cells
Round
Spindle
Flat
n=294
n=364
n=305
n=287
n=310
n=256
1 2 3 4 5 6

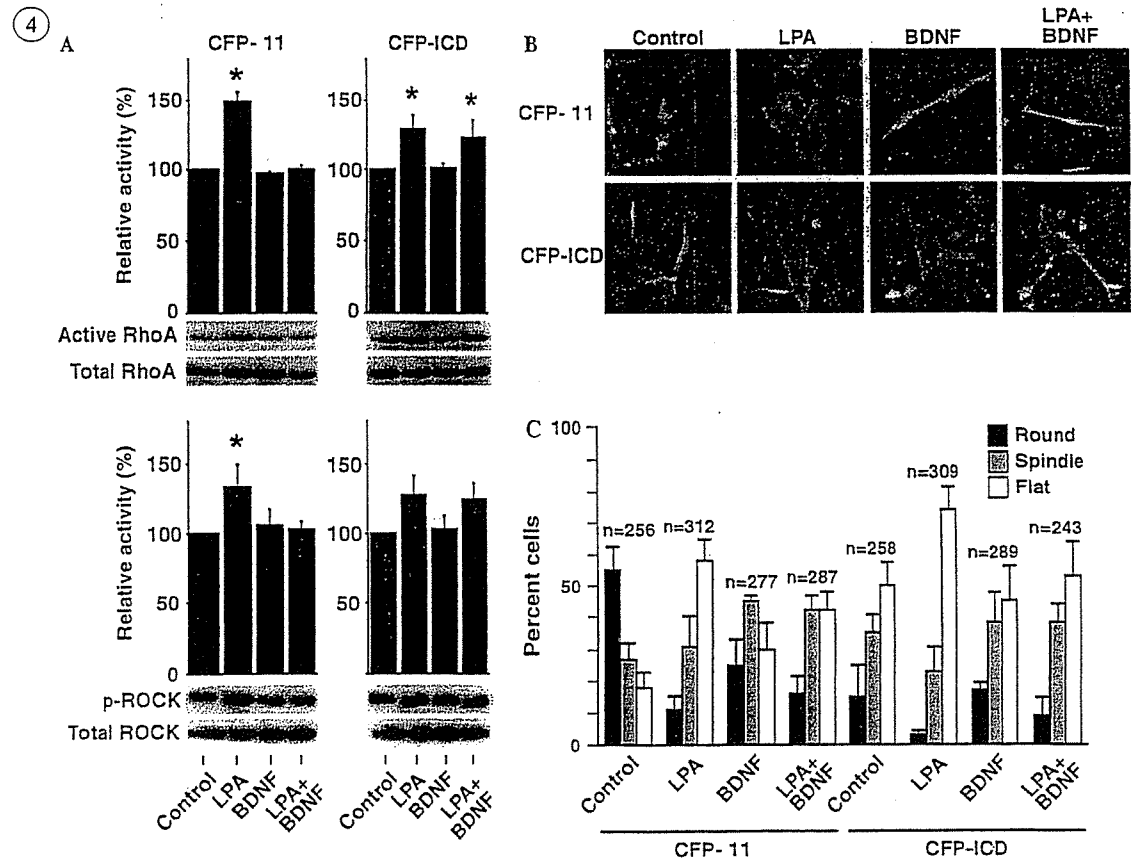
4
A
CFP- 11
CFP-ICD
Relative activity (%)
Active RhoA
Total RhoA
p-ROCK
Total ROCK
Control
LPA
BDNF
LPA+ BDNF
B
Control
LPA
BDNF
LPA+ BDNF
CFP- 11
CFP-ICD
C
Percent cells
Round
Spindle
Flat
n=256
n=312
n=277
n=287
n=258
n=309
n=289
n=243
CFP- 11
CFP-ICD

by LPA treatment (10 μM) (Fig. 3A), while BDNF alone did not alter the phosphorylation of ROCK. On the other hand, the LPA-induced phosphorylation of ROCK was reduced to the control level by BDNF stimulation. Thus, ROCK activity was found to correlate with RhoA activity in the present study.

Recently, it has been reported that p75 associates with Rho GDI1 and regulates Rho activity [28]. In order to examine the contribution of p75 in the present experiment, cells were incubated during operations with an anti-p75 antibody, clone MC192, which inhibits the interaction between p75 and Trk receptors [15,29]. If there were a contribution of p75 in the present experiment, the activities of RhoA and ROCK would be maintained at a high level in the cells treated by LPA + BDNF, that is, when BDNF action is inhibited. However, we found that the anti-p75 antibody treatment had no effect on BDNF action, which reduced the high activity levels of RhoA and ROCK induced by LPA (Fig. 3A, lane 6). Therefore, it is unlikely that p75 contributed to the regulation of Rho proteins in our experiment.

Changes in C6 cell morphology due to T1-Rho GDI1

It is known that Rho proteins can regulate cell morphology via remodeling of the actin cytoskeleton [30]. Thus, we examined the effect of BDNF on cell morphology and on the reorganization of the actin cytoskeleton. C6 cells tended to show a rounded shape and modest stress fiber staining in the cell periphery in the control samples (Figs. 3B and C). In contrast, LPA (10 μM)-treated cells showed a flattened shape (68%) and strong stress fiber bundles. When cells were treated with BDNF (20 ng/ml), the percentage of spindle-shaped cells (48%) was greater than that of the control (26%) and that of LPA-treated (29%) cells. We next examined whether the LPA-induced production of stress fibers could be blocked by BDNF stimulation. The cells were first treated with LPA for 30 min and then incubated with BDNF for 30 min. Subsequent staining of the cells showed fewer or no stress fibers. In addition, the percentage of spindle-shaped cells increased from 29% to 48%, while that of flat-shaped cells decreased from 68% to 45% compared with the LPA-treated cells. Furthermore, anti-BDNF antibody was able to inhibit the BDNF action, suggesting that this effect is BDNF-specific. On the other hand, anti-p75 antibody did not inhibit the effect of BDNF on cell morphology and actin remodeling, suggesting that p75 is not involved in the regulation of cell morphology or actin remodeling.

Competitive assay with T1 intracellular peptides

To further examine the inhibitory effect of the intracellular domain of T1 for Rho signaling, we carried out the transfection of the pCFP-intracellular domain of T1, CFP-Δ11, and CFP-ICD, in order to inhibit the T1 signaling cascade in a competitive manner. We expected that CFP-ICD, but not CFP or CFP-Δ11, would trap Rho GDI1 within the cytoplasmic region and inhibit the association of Rho GDI1 with the Rho GTPases, thereby resulting in the inhibition of the BDNF effect. When CFP (data not shown) and CFP-Δ11 were expressed, the changes in cell morphology were comparable with those of untransfected cells (Figs. 3 and 4), suggesting that the first 12 intracellular amino acids of T1 are not affected by changes in C6 cell morphology. In contrast, the cells expressing CFP-ICD showed spindle or flat shapes even under no treatment conditions. Moreover, the CFP-ICD was able to reduce the BDNF effect which transforms a flat cell into a spindle-shaped cell, suggesting that the T1-specific sequence is important in BDNF-dependent C6 morphological regulation.

Control of the PAK-signaling cascade by T1

Recently, Rho family proteins have been reported to upregulate the PAK activity that is involved in the regulation of axon growth [31], which can activate both Raf and mitogen-activated protein kinase (MEK), leading to ERK activation [32–34]. Thus, to confirm that T1-Rho GDI1 signaling could regulate the other effectors of Rho proteins, we examined whether T1 regulates the phosphorylation of PAK and ERK. Phosphorylated PAK was significantly

Fig. 3. Regulation of the Rho-signaling cascade and morphological changes in C6 cells. 1, control; 2, BDNF (10 ng/ml); 3, LPA (10 μM); 4, LPA + BDNF; 5, anti-BDNF (5 μg/ml) + BDNF; 6, MC192 (1/50 of culture medium) + LPA + BDNF. (A) Analysis of RhoA and ROCK activities in C6 cells. Control levels were taken as 100%. The asterisks indicate significant differences ($p < 0.05$ by one-way analysis of variance (ANOVA) and Scheffé's post hoc test) compared to control levels. Values are given as means ± SD and are the result of four independent experiments. (B) Confocal microscopic images. Green (FITC-phalloidin) and red (propidium iodide) represent actin fibers and cell nuclei, respectively. All panels are merged images. In Image 1, three types of cell morphology are seen: arrowhead, round type; double-arrowhead spindle type; arrow, flat type. Scale bar, 30 μm. (C) Populations of the three categories of cell morphology. Values are given as means ± SD of four independent experiments. The numbers indicate the total cell counts.

Fig. 4. Competitive assay using the fusion proteins of CFP and specific peptides of T1. (A) Analysis of RhoA and ROCK activities in C6 cells with CFP-Δ11 and CFP-ICD having been transfected. Control levels were taken as 100%. The asterisks indicate significant differences ($p < 0.05$ by one-way ANOVA and Scheffé's post hoc test) from the levels of the controls. Values are given as means ± SD and are the result of four independent experiments. (B) Confocal microscopic images of changes in the morphology and stress fibers of C6 cells. Green (FITC-phalloidin), red (propidium iodide), and blue (CFP) represent actin fibers, cell bodies, and overexpressing CFP-fusion proteins, respectively. All panels are merged images. Scale bar, 30 μm. (C) Populations of the three categories of cell morphology. Values are given as means ± SD and are the result of four independent experiments. The numbers indicate the total cell counts.

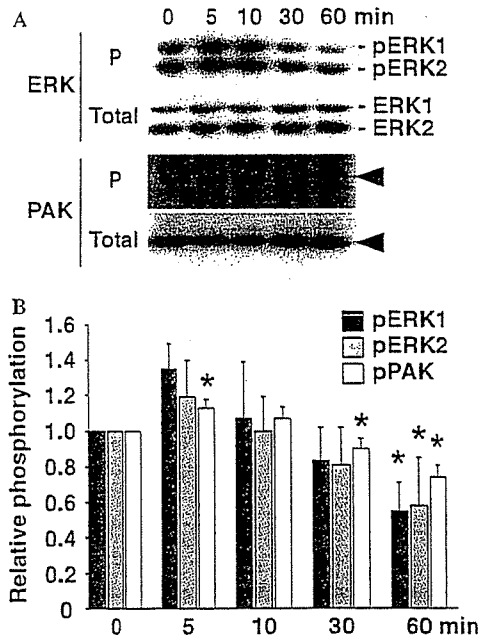

Fig. 5. Phosphorylation of PAK and ERK1/2 in C6 cells. (A) Western blot analysis of PAK and ERK1/2 phosphorylation. P indicates phosphorylated proteins. (B) Quantitative analysis of the bands in (A). The asterisks indicate values that were significantly different ($p < 0.05$ by one-way ANOVA and Scheffé's post hoc test) from control values. The results of four experiments are shown as means ± SD. The horizontal axis shows the progress time after BDNF administration, and the vertical axis shows the percentage of phosphorylation. The levels at 0 min were taken as 100%.

increased up to 113% by BDNF stimulation at 5 min and significantly decreased to 88% and 75% of the control levels at 30 and 60 min, respectively (Fig. 5). Following an increase of phosphorylated ERK1/2 after BDNF stimulation, the phosphorylated ERK1/2, albeit not significantly, decreased to below control levels within 30 min (ERK1, 80%; ERK2, 77%) and was significantly reduced to approximately 60% of control levels at 60 min (ERK1, 57%; ERK2, 60%). Together, the activities of PAK and ERK were well correlated with those of RhoA and ROCK, suggesting that T1-Rho GDI1 signaling may regulate PAK and ERK activities.

Discussion

In the present study, we demonstrated that a truncated TrkB receptor, T1, is capable of ligand-mediated signaling through the T1- Rho GDI1 pathway, which acts negatively for Rho and ERK-signaling cascades in a BDNF-dependent manner, and that T1-Rho GDI1 signaling regulates the cellular morphology of glioma cells via remodeling of the actin cytoskeleton.

Control of Rho signaling and cell morphology by T1

The present results provide evidence that T1 signaling can negatively regulate the Rho and PAK-signaling pathways in a ligand-dependent manner. The substrates of Rho GDI1 are RhoA and -B, Rac1 and -2, and Cdc42. ROCK, a target protein of Rho, is involved in the formation of stress fiber and axon growth [35]. On the other hand, PAK plays an important role in actin remodeling for membrane ruffles and lamellipodium, and in the axon growth of neurons [31,36,37]. Thus, T1 signaling may cease the reorganization of the actin cytoskeleton. In addition, Rho proteins have been reported to regulate microtubules and intermediate filaments [30], suggesting that cell morphology may be determined by other such cytoskeleton elements.

The importance of the control of Rho proteins and the cytoskeleton by T1-Rho GDI1 signaling is hinted in a recent study by Horch et al. [38]. In their paper, they demonstrate that BDNF stimulation induces structural instability in dendrites and spines of neurons in the ferret visual cortex on postnatal days 25–28 [38], when T1 has already expressed in the ferret cerebral cortex [11]. Thus, the instability of dendrites and spines that might be induced by T1 may be attributed in part to preparation for the next morphological changes in cells.

The relationship between Rho proteins and cell morphology is more complicated than we tend to assume. For example, in mammalian neuroblastoma cells, Rho inhibits neurite outgrowth, while both Rac and Cdc42 promote neurite outgrowth [39,40]. However, in chick dorsal root ganglion neurons, the opposite occurs [41]. Therefore, the subcellular localization of Rho family proteins and T1 and/or the compositional rate of Rho proteins and their targets may determine how remodeling of the cytoskeleton occurs and thus how cells alter their shapes.

Control of ERK and PAK by T1

In the present study, we observed the upregulation of PAK and ERK1/2 phosphorylation within 5 min. This result was different from our expectations. One possible mechanism by which the phosphorylation of PAK and ERK is activated may involve the participation of low contents of TK+, which activates ERK1/2 via Ras-Raf-MEK1. The phosphorylation of ERK1/2 has been reported to be a very rapid reaction that occurs within 5 min [42]. There are two pathways by which ERK1/2 is activated, namely, the Ras- and Rho-dependent pathways, which converge on the Raf and MEK levels [32,34]. Therefore, after the activation of ERK by Rho signaling is stopped by Rho GDI1, the dephosphorylation of ERK1/2 by the endogenous phosphatases might be faster than the phosphorylation of ERK1/2 by Ras signaling. Consequently, the phosphorylation levels of ERK1/2 may decrease.

ERK1/2 is generally implicated in the regulation of growth responses of cells. It is of note that T1 has an inhibitory effect on ERK activation in C6 cells, while

TK+ can activate ERK1/2 via Ras. Therefore, T1 might cooperate with TK+ to confine BDNF functions spatiotemporally.

Acknowledgments

The authors thank Dr. Hans Thoenen for his helpful suggestions and comments. This work was supported by grants from the Ministry of Education, Culture, Sports, Science and Technology of Japan [No. 15016056 to M.H., No. 16015341 to S.N., Biodiversity Research of 21st Century COE (A14)], and the Organization of Pharmaceutical Safety and Research (Nano-1).

References

[1] M. Barbacid, The Trk family of neurotrophin receptors, J. Neurobiol. 25 (1994) 1386–1403.
[2] Q. Yan, M.J. Radeke, C.R. Matheson, J. Talvenheimo, A.A. Welcher, S.C. Feinstein, Immunocytochemical localization of TrkB in the central nervous system of the adult rat, J. Comp. Neurol. 378 (1997) 135–157.
[3] Q. Yan, R.D. Rosenfeld, C.R. Matheson, N. Hawkins, O.T. Lopez, L. Bennet, A.A. Welcher, Expression of brain-derived neurotrophic factor protein in the adult rat central nervous system, Neuroscience 78 (1997) 431–448.
[4] K. Ohira, K. Shimizu, M. Hayashi, Change of expression of full-length and truncated TrkBs in the developing monkey central nervous system, Dev. Brain Res. 112 (1999) 21–29.
[5] M. Bibel, Y.A. Barde, Neurotrophins: key regulators of cell fate and cell shapes in the vertebrate nervous system, Genes Dev. 14 (2000) 2919–2937.
[6] H. Thoenen, Neurotrophins and activity-dependent plasticity, Prog. Brain Res. 128 (2000) 183–191.
[7] R.A. Segal, Selectivity in neurotrophin signaling: theme and variations, Annu. Rev. Neurosci. 26 (2003) 299–330.
[8] R. Klein, D. Conway, L.F. Parada, M. Barbacid, The trkB tyrosine kinase gene codes for a second neurogenic receptor that lacks the catalytic kinase domain, Cell 61 (1990) 647–656.
[9] D.S. Middlemas, R.A. Lindberg, T. Hunter, TrkB, a neural receptor protein-tyrosine kinase: evidence for a full-length and two truncated receptors, Mol. Cell. Biol. 11 (1991) 143–153.
[10] D.L. Shelton, J. Sutherland, J. Gripp, T. Camerato, M.P. Armanini, H.S. Phillips, K. Carroll, S.D. Spencer, A.D. Levinson, Human trks: molecular cloning, tissue distribution, and expression of extracellular domain immunoadhesins, J. Neurosci. 15 (1995) 477–491.
[11] K.L. Allendoerfer, R.J. Cabelli, E. Escandon, D.R. Kaplan, K. Nikolics, C.J. Shatz, Regulation of neurotrophin receptors during the maturation of the mammalian visual system, J. Neurosci. 14 (1994) 1795–1811.
[12] R.H. Fryer, D.R. Kaplan, S.C. Feinstein, M.J. Radeke, D.R. Grayson, L.F. Kromer, Developmental and mature expression of full-length and truncated TrkB receptors in the rat forebrain, J. Comp. Neurol. 374 (1996) 21–40.
[13] K. Ohira, K. Shimizu, M. Hayashi, TrkB dimerization during development of the prefrontal cortex of the macaque, J. Neurosci. Res. 65 (2001) 463–469.
[14] T.A. Yacoubian, D.C. Lo, Truncated and full-length TrkB receptors regulate distinct modes of dendritic growth, Nat. Neurosci. 3 (2000) 342–349.
[15] M. Hartmann, T. Brigadski, K.S. Erdmann, B. Holtmann, M. Sendtner, F. Narz, V. Leßmann, Truncated TrkB receptor-induced outgrowth of dendritic filopodia involves the p75 neurotrophin receptor, J. Cell Sci. 117 (2004) 5803–5814.
[16] K. Ohira, H. Kumanogoh, Y. Sahara, K.J. Homma, H. Hirai, S. Nakamura, M. Hayashi, A truncated TrkB receptor, T1, regulates glial cell morphology via Rho GDP dissociation inhibitor 1, J. Neurosci. 25 (2005) 1343–1353.
[17] K. Ohira, K. Shimizu, A. Yamashita, M. Hayashi, Differential expression of the truncated TrkB receptor, T1, in the primary motor and prefrontal cortices of the adult macaque monkey, Neurosci. Lett. 385 (2005) 105–109.
[18] C.R. Rose, R. Blum, B. Pichler, A. Lepier, K.W. Kafitz, A. Konnerth, Truncated TrkB-T1 mediates neurotrophin-evoked calcium signalling in glia cells, Nature 426 (2003) 74–78.
[19] Y. Takai, T. Sasaki, T. Matozaki, Small GTP-binding proteins, Physiol. Rev. 81 (2001) 153–208.
[20] X.D. Ren, W.B. Kiosses, M.A. Schwartz, Regulation of the small GTP-binding protein Rho by cell adhesion and the cytoskeleton, EMBO J. 18 (1999) 578–585.
[21] K. Ohira, M. Hayashi, Expression of TrkB subtypes in the adult monkey cerebellar cortex, J. Chem. Neuroanat. 25 (2003) 175–183.
[22] K. Ohira, N. Funatsu, S. Nakamura, M. Hayashi, Expression of BDNF and TrkB receptor subtypes in the postnatal developing Purkinje cells of monkey cerebellum, Gene Expr. Patterns 4 (2004) 257–261.
[23] H. Hirai, P.T. LoVerde, FISH techniques for constructing physical maps on schistosome chromosomes, Parasitol. Today 11 (1995) 310–314.
[24] M.P. Armanini, S.B. McMahon, J. Sutherland, D.L. Shelton, H.S. Phillips, Truncated and catalytic isoforms of trkB are co-expressed in neurons of rat and mouse CNS, Eur. J. Neurosci. 7 (1995) 1403–1409.
[25] S. Yoshimura, H. Sakai, S. Nakashima, Y. Nozawa, J. Shinoda, N. Sakai, H. Yamada, Differential expression of Rho family GTP-binding proteins and protein kinase C isozymes during C6 glial cell differentiation, Mol. Brain Res. 45 (1997) 90–98.
[26] M. Maekawa, T. Ishizaki, S. Boku, N. Watanabe, A. Fujita, A. Iwamatsu, T. Obinata, K. Ohashi, K. Mizuno, S. Narumiya, Signaling from Rho to the actin cytoskeleton through protein kinases ROCK and LIM-kinase, Science 285 (1999) 895–898.
[27] A.L. Bishop, A. Hall, Rho GTPases and their effector proteins, Biochem. J. 348 (2000) 241–255.
[28] T. Yamashita, M. Tohyama, The p75 receptor acts as a displacement factor that releases Rho from Rho-GDI, Nat. Neurosci. 6 (2003) 436–461.
[29] P.A. Barker, E.M. Shooter, Disruption of NGF binding to the low affinity neurotrophin receptor p75LNTR reduces NGF binding to TrkA on PC12 cells, Neuron 13 (1994) 203–215.
[30] S. Etienne-Manneville, A. Hall, Rho GTPases in cell biology, Nature 420 (2002) 629–635.
[31] J. Ng, L. Luo, Rho GTPases regulate axon growth through convergent and divergent signaling pathways, Neuron 44 (2004) 779–793.
[32] J.A. Frost, H. Steen, P. Shapiro, T. Lewis, N. Ahn, P.E. Shaw, M.H. Cobb, Cross-cascade activation of ERKs and ternary complex factors by Rho family proteins, EMBO J. 21 (1997) 6426–6438.
[33] A.J. King, H. Sun, B. Diaz, D. Barnard, W. Miao, S. Bagrodia, M.S. Marshall, The protein kinase Pak3 positively regulates Raf-1 activity through phosphorylation of serine 338, Nature 396 (1998) 180–183.
[34] A. Clerk, F.H. Pham, S.J. Fuller, E. Sahai, K. Aktories, R. Marais, C. Marshall, P.H. Sugden, Regulation of mitogen-activated protein kinases in cardiac myocytes through the small G protein Rac1, Mol. Cell. Biol. 21 (2001) 1173–1184.
[35] H. Bito, T. Furuyashiki, H. Ishihara, Y. Shibasaki, K. Ohashi, K. Mizuno, M. Maekawa, T. Ishizaki, S. Narumiya, A critical role for a Rho-associated kinase, p160ROCK, in determining axon outgrowth in mammalian CNS neurons, Neuron 26 (2000) 431–441.
[36] E. Manser, H.Y. Huang, T.H. Loo, X.Q. Chen, J.M. Dong, T. Leung, L. Lim, Expression of constitutively active alpha-PAK reveals effects of the kinase on actin and focal complexes, Mol. Cell. Biol. 17 (1997) 1129–1143.

[37] M.A. Sells, U.G. Knaus, S. Bagrodia, D.M. Ambrose, G.M. Bokoch, J. Chernoff, Human p21-activated kinase (Pak1) regulates actin organization in mammalian cells, Curr. Biol. 7 (1997) 202–210.
[38] H.W. Horch, A. Kruttgen, S.D. Portbury, L.C. Katz, Destabilization of cortical dendrites and spines by BDNF, Neuron 23 (1999) 353–364.
[39] R. Kozma, S. Samer, S. Ahmed, L. Lim, Rho family GTPases and neuronal growth cone remodelling: relationship between increased complexity induced by Cdc42Hs, Rac1, and acetylcholine and collapse induced by RhoA and lysophosphatidic acid, Mol. Cell. Biol. 17 (1997) 1201–1211.
[40] M. Hirose, T. Ishizaki, N. Watanabe, M. Uehata, O. Kranenburg, W.H. Moolenaar, F. Matsumura, M. Maekawa, H. Bito, S. Narumiya, Molecular dissection of the Rho-associated protein kinase (p160ROCK)-regulated neurite remodeling in neuroblastoma N1E-115 cells, J. Cell Biol. 141 (1998) 1625–1636.
[41] Z. Jin, S.M. Strittmatter, Rac1 mediates collapsin-1-induced growth cone collapse, J. Neurosci. 17 (1997) 6256–6263.
[42] H.N. Marsh, W.K. Scholz, F. Lamballe, R. Klein, V. Nanduri, M. Barbacid, H.C. Palfrey, Signal transduction events mediated by the BDNF receptor gp145trkB in primary hippocampal pyramidal cell culture, J. Neurosci. 13 (1993) 4281–4292.

Ubiquitin C-terminal hydrolase L1 regulates the morphology of neural progenitor cells and modulates their differentiation

Mikako Sakurai[1,2], Koichi Ayukawa[1], Rieko Setsuie[1,2], Kaori Nishikawa[1], Yoko Hara[1], Hiroki Ohashi[1,3], Mika Nishimoto[1,4], Toshiaki Abe[3], Yoshihisa Kudo[4], Masayuki Sekiguchi[1], Yae Sato[1,2], Shunsuke Aoki[1], Mami Noda[2] and Keiji Wada[1,*]

[1]Department of Degenerative Neurological Diseases, National Institute of Neuroscience, National Center of Neurology and Psychiatry, Kodaira, Tokyo, 187-8502, Japan
[2]Laboratory of Pathophysiology, Graduate School of Pharmaceutical Sciences, Kyushu University, Higashi-ku, Fukuoka, 812-8582, Japan
[3]Department of Neurosurgery, Graduate School of Medicine, Jikei University School of Medicine, Minato-ku, Tokyo, 105-8461, Japan
[4]Laboratory of Cellular Neurobiology, Tokyo University of Pharmacy and Life Science, Hachioji, Tokyo, 192-0392, Japan
*Author for correspondence (e-mail: wada@ncnp.go.jp)

Accepted 27 September 2005
Journal of Cell Science 119, 162-171 Published by The Company of Biologists 2006
doi:10.1242/jcs.02716

Summary

Ubiquitin C-terminal hydrolase L1 (UCH-L1) is a component of the ubiquitin system, which has a fundamental role in regulating various biological activities. However, the functional role of the ubiquitin system in neurogenesis is not known. Here we show that UCH-L1 regulates the morphology of neural progenitor cells (NPCs) and mediates neurogenesis. UCH-L1 was expressed in cultured NPCs as well as in embryonic brain. Its expression pattern in the ventricular zone (VZ) changed between embryonic day (E) 14 and E16, which corresponds to the transition from neurogenesis to gliogenesis. At E14, UCH-L1 was highly expressed in the ventricular zone, where neurogenesis actively occurs; whereas its expression was prominent in the cortical plate at E16. UCH-L1 was very weakly detected in the VZ at E16, which corresponds to the start of gliogenesis. In cultured proliferating NPCs, UCH-L1 was co-expressed with nestin, a marker of undifferentiated cells. In differentiating cells, UCH-L1 was highly co-expressed with the early neuronal marker TuJ1. Furthermore, when UCH-L1 was induced in nestin-positive progenitor cells, the number and length of cellular processes of the progenitors decreased, suggesting that the progenitor cells were differentiating. In addition, NPCs derived from *gad* (UCH-L1-deficient) mice had longer processes compared with controls. The ability of UCH-L1 to regulate the morphology of nestin-positive progenitors was dependent on its binding affinity for ubiquitin but not on hydrolase activity; this result was also confirmed using *gad*-mouse-derived NPCs. These results suggest that UCH-L1 spatially mediates and enhances neurogenesis in the embryonic brain by regulating progenitor cell morphology.

Key words: PGP9.5, UCH-L1, Nestin, Ubiquitin, Cell morphology, Differentiation, Progenitor

Introduction

Ubiquitin C-terminal hydrolase L1 (UCH-L1) is a member of the deubiquitylating enzymes and is one of the most abundant proteins in the brain. Whereas other UCH members are ubiquitously expressed, UCH-L1 is selectively expressed in neurons and testes/ovaries in the adult (Wilkinson et al., 1989). UCH-L1 is also known as PGP9.5 and is used as a neuron-specific marker in neuroanatomical and neuropathological studies (Dickson et al., 1994; McQuaid et al., 1995). Recent studies suggest that UCH-L1 is involved in neurodegeneration. The I93M mutation and the S18Y polymorphism in UCH-L1 are implicated in Parkinson's disease (Leroy et al., 1998; Satoh and Kuroda, 2001). Using gracile axonal dystrophy (*gad*) mice, we previously demonstrated that the dying-back type of axonal degeneration is caused by a deletion of the *Uchl1* gene (Saigoh et al., 1999). UCH-L1 has an affinity for ubiquitin and ensures its stability within neurons in vivo (Osaka et al., 2003). Furthermore, UCH-L1 has ubiquitin ligase activity (Liu et al., 2002). Thus, UCH-L1 might have multiple functions and more roles in biological phenomena than previously expected.

UCH-L1 mRNA is first detected at embryonic day (E) 8.5-9 in the neural tube and in the neural epithelium (Schofield et al., 1995). In addition, UCH-L1 immunoreactivity has been observed in the neural tube at E10.5 (Sekiguchi et al., 2003). However, its functional role in embryonic neurogenesis is not well understood. CDK5 and Dab1 are involved in regulating the migratory behavior of postmitotic neurons. Both p35, which is a CDK5 kinase, and Dab1 are degraded by the ubiquitin-proteasome pathway (Arnaud et al., 2003; Bock et al., 2004; Patrick et al., 1998). Thus, the ubiquitin system might be important in the migration and differentiation of postmitotic neurons and for the lamination pattern of the cerebral cortex.

Neural progenitor cells (NPCs) differentiate into neurons, astrocytes and oligodendrocytes (Qian et al., 1998; Qian et al., 2000; Shen et al., 1998). In the embryonic brain, neuroepithelial cells and radial glia are present in the ventricular zone (VZ); neurogenesis occurs first, followed by

gliogenesis. Committed progenitor cells move from the VZ to the cortical plate (CP) (Noctor et al., 2004). The differentiating cells migrate by means of radial migration, during which the migrating cells change their morphology (Kawauchi et al., 2003; Noctor et al., 2002; Tabata and Nakajima, 2003). Here, we analyzed the functional role of UCH-L1 using mouse embryonic NPCs. Our results indicate that UCH-L1 is expressed in nestin-positive NPCs and might regulate neurogenesis. The expression pattern of UCH-L1 changed in parallel with the transition from neuronal generation to glial generation. Furthermore, UCH-L1 modulated the length of nestin-positive processes in NPCs. Our results constitute the first evidence that UCH-L1 is important in neurogenesis and thus provide the basis for further investigation into the role of the ubiquitin system in neurogenesis.

Results

UCH-L1 expression in embryonic mouse brain

We first determined the specificity of the UCH-L1 antibody using immunoblotting (data not shown) and immunostaining. Because *gad* mice do not express endogenous UCH-L1 (Saigoh et al., 1999), we used these mice as a negative control. Heterozygous littermates had UCH-L1 immunostaining, whereas UCH-L1 immunoreactivity was not detected in the brains of *gad* mice (Fig. 1). These results confirmed the specificity of the antibody against UCH-L1. Using this antibody, we further compared the distribution and expression of UCH-L1 with the neural progenitor marker nestin and the early neuronal marker TuJ1. Nestin was expressed in the VZ of brains from both *gad* and heterozygous mice at E13 (Fig. 1). Nestin expression was observed throughout the region, whereas TuJ1 immunoreactivity was detected at the marginal zone (MZ). In heterozygous mice, UCH-L1 and nestin immunostaining overlapped in almost all cells in the VZ, suggesting that UCH-L1 is expressed in NPCs (Fig. 1A). TuJ1 expression colocalized with that of UCH-L1 in MZ cells, indicating that UCH-L1 is expressed in embryonic neurons as well (Fig. 1B). In E13 *gad* mouse brain, nestin staining differed compared with that in heterozygous littermates. Nestin staining was observed in many long radial fibers in the mutant, which we believed were radial glia; by contrast, staining in the heterozygotes occurred in radial glia as well as in neuronal cells at various stages of development (Fig. 1A; arrow and arrowhead).

We then looked for developmental changes in UCH-L1 expression. In the embryonic cerebral cortex, asymmetric cell division generates one neuron and one neural progenitor (Roegiers and Jan, 2004; Zhong et al., 1996; Zhong et al., 1997). These asymmetric cell divisions begin at E11, peak around E14, and subside after E16. At E14, astrocytes and oligodendrocytes are not yet present. However, at E16, glial cell production begins. The regional expression level for both nestin and TuJ1 did not change between E14 and E16 (Fig. 2A,B). At E14 and E16, nestin immunoreactivity was stronger in the VZ (Fig. 2A) and was faintly detected only along radial glial fibers in the CP (Fig. 2A,C; arrowhead) (Malatesta et al., 2003; Malatesta et al., 2000). TuJ1 immunoreactivity was predominantly detected in the MZ, CP, intermediate zone and subventricular zone at E14 and E16 (Fig. 2B,D). In the VZ, TuJ1 immunoreactivity was detected only in migrating neurons (Fig. 2D; arrowhead).

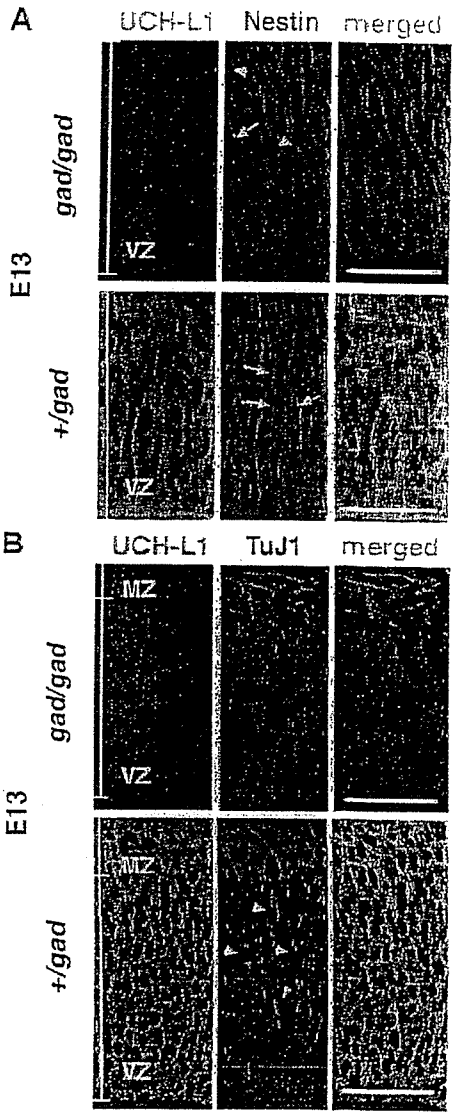

Fig. 1. Antibody specificity and expression of UCH-L1 in the ventricular zone at E13. UCH-L1 expression was detected using immunohistochemistry with anti-PGP9.5. UCH-L1 is not detected in the brain of *gad* mice at E13 (A,B) but is strongly expressed in heterozygous littermates (A,B). Confocal microscopic images of coronal sections of *gad* mice and heterozygous littermates were double stained with antibodies for the progenitor marker nestin and UCH-L1 (PGP9.5) (A) or for the early neuronal marker tubulin β III (TuJ1) and UCH-L1 (B). Long radial fibers are indicated by arrowheads, and various phases of progenitor cells are indicated by arrows (A). TuJ1-positive, migrating neuronal cells are indicated by arrowheads (B). MZ, marginal zone; VZ, ventricular zone. Bars, 40 μm.

By contrast, the pattern of UCH-L1 expression changed between E14 and E16 (Fig. 2A,B). At both stages of development, UCH-L1 was expressed in neuronal cells as well as in progenitor cells. UCH-L1 immunoreactivity was stronger in the VZ than in the CP at E14; however, the immunoreactivity

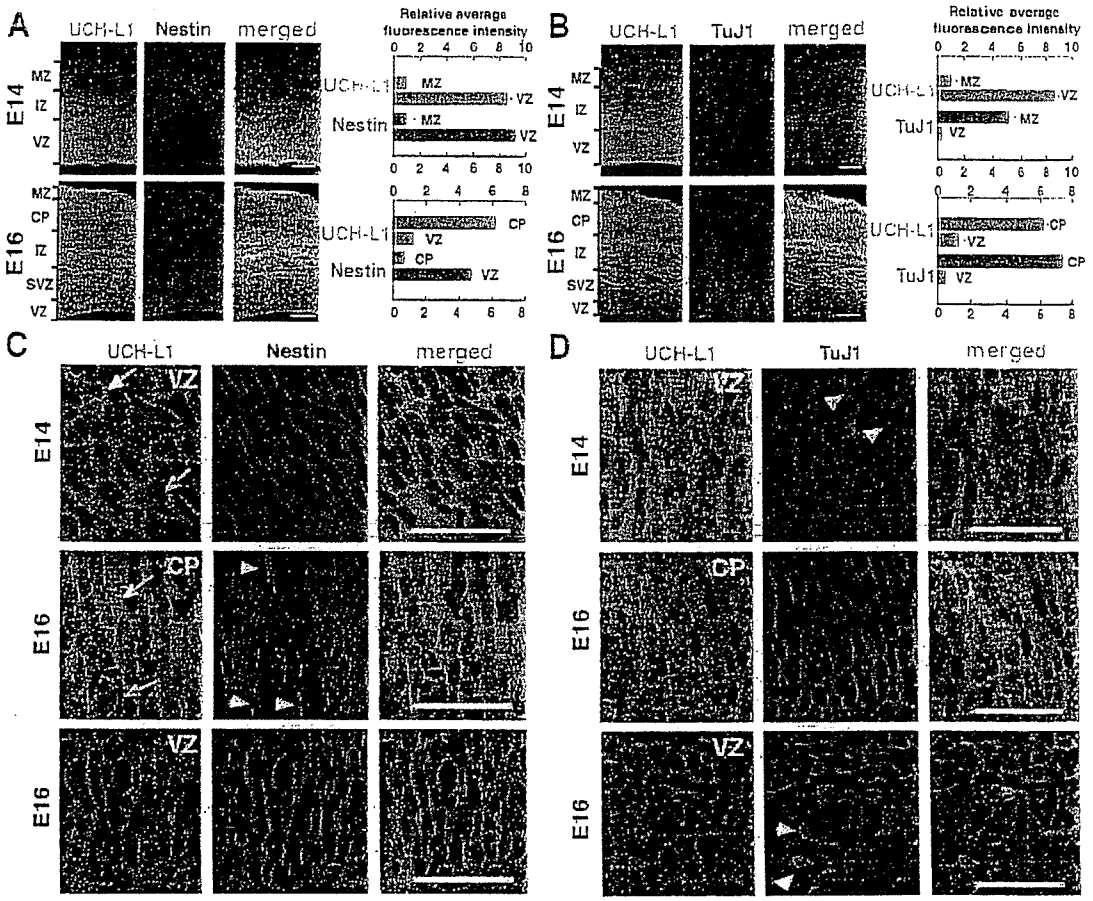

Fig. 2. Change in UCH-L1 expression pattern in the developing mouse brain. Cryosections of the brain at E14 and E16 were double stained with UCH-L1 and the neural progenitor marker nestin (A) or early neuronal marker TuJ1 (B). Unlike with UCH-L1, staining patterns for TuJ1 and nestin do not change between E14 and E16. At E14, UCH-L1 expression is higher in the VZ than in the MZ. At E16, higher expression of UCH-L1 is reciprocally detected in the CP. By contrast, at both E14 and E16, nestin is highly expressed in the VZ, and TuJ1 expression is higher in the MZ/CP. Fluorescence intensities per field (1700 μm^2) were measured in each layer of the E14 and E16 brain and are shown to the right. Bars, 80 μm. (C,D) Higher-magnification images from A,B of UCH-L1 expression in the E14 and E16 brain: UCH-L1 and nestin (C); UCH-L1 and TuJ1 (D). UCH-L1 and nestin are co-expressed in the VZ at E14 and E16. Nestin is expressed only in radial glial fibers (arrowheads) of the CP but not in neurons. UCH-L1 expression level is high. A representative cell with a high level of UCH-L1 expression is indicated by a white arrow and one with low expression is indicated by a yellow arrow (C). An early neuronal marker, TuJ1, was expressed in both migrating (arrowheads) and mature neurons (D). CP, cortical plate; IZ, intermediate zone; MZ, marginal zone; SVZ, subventricular zone; VZ, ventricular zone. Bars, 40 μm.

was stronger in the CP than in the VZ at E16 (Fig. 2A,B). The regional change in UCH-L1 expression between E14 and E16 was further confirmed by measuring immunofluorescence intensities from confocal images of the MZ/CP and VZ. At E14, the relative UCH-L1 expression level in the VZ was 9.3 times higher than that in the MZ (Fig. 2A).

Conversely, at E16, when neuronal maturation occurs in the CP, UCH-L1 immunoreactivity in the CP was 5.0 times higher than in the VZ (Fig. 2B). UCH-L1 immunoreactivity colocalized with that of nestin in the VZ at both E14 and E16, although UCH-L1 expression in the VZ was lower at E16 (Fig. 2C). In the VZ at E14, nestin was expressed homogeneously; however, the pattern of UCH-L1 immunoreactivity was mixed, with strong and weak intensities (Fig. 2C; arrow). This expression pattern might reflect the heterogeneity of progenitor cells. Nestin-positive radial glial fibers were observed in the CP at E16 through mature neurons, which strongly expressed UCH-L1 (Fig. 2C) (Malatesta et al., 2000; Malatesta et al., 2003).

UCH-L1 and nestin expression in cultured NPCs

Because areas of nestin and UCH-L1 immunoreactivity overlapped in the VZ, where NPCs reside, we subsequently analyzed the transition of UCH-L1 expression using cultured NPCs. We performed double-labeling experiments for UCH-L1 and nestin expression in cultured NPCs. In the presence of basic fibroblast growth factor (bFGF), when NPCs are proliferating, the percentage of UCH-L1/nestin double-positive

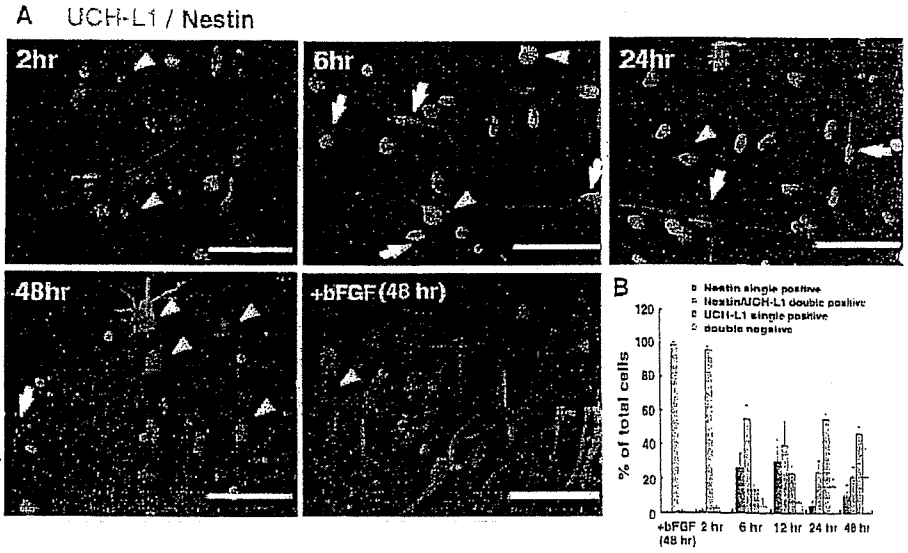

Fig. 3. Nestin and UCH-L1 expression in undifferentiated and differentiating NPCs at 2, 6, 12, 24 and 48 hours. (A) NPCs were immunolabeled with antibodies against nestin and UCH-L1 in the proliferating phase (+bFGF; at 48 hours) or the differentiation phase (–bFGF; 2, 6, 24, 48 hours). Cultures were counterlabeled with Hoechst nuclear dye to facilitate cell quantification. (B) Quantitative analysis of the percentage of cells stained with each antibody. Nestin-positive cells gradually decrease as differentiation proceeds. The UCH-L1 expression level is both high (arrowheads) and low (arrows) in nestin-positive cells at 6 hours. Each experiment was analyzed by counting cells in three independent wells at the indicated times. The experiments were repeated at least two times. Bars, 50 μm.

cells did not change 48 hours after plating, and almost all NPCs expressed UCH-L1 (Fig. 3A). The majority (97.5±2.2%; mean±s.d.) of cultured cells were nestin positive and most of them also stained for UCH-L1 2 hours after plating without bFGF, which triggers NPC differentiation. UCH-L1/nestin double-positive cells were detected at all time points, but as differentiation proceeded their numbers gradually decreased from 95.8±1.9% at 2 hours to 21.5±5.8% at 48 hours (Fig. 3A,B). Although UCH-L1 single-positive cells were rarely detected at 2 hours, the population increased with differentiation, and by 24 hours after bFGF removal 55.1±2.9% of cultured cells were UCH-L1 single-positive cells. Conversely, nestin single-positive cells were readily detected during the earlier phase of differentiation, especially at 6 hours (26.4±8.4% of total cells) and 12 hours (27.0±14.0% of total cells). The differentiating NPCs included nestin-positive cells in which UCH-L1 was either strongly or weakly expressed (Fig. 3A; arrow and arrowhead at 6 hours). These data indicate that UCH-L1 is expressed in progenitor cells as well as in differentiating NPCs. Nestin-positive cells can probably be

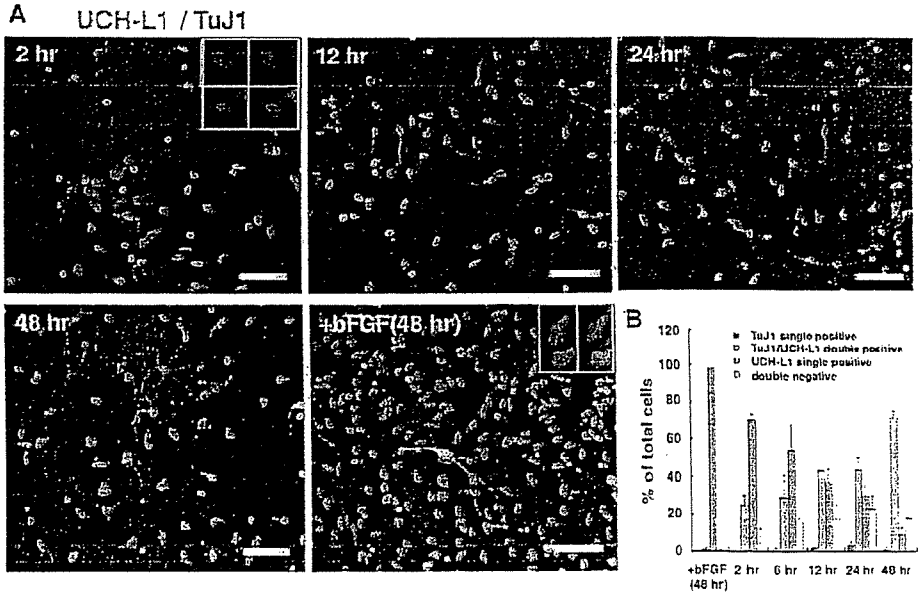

Fig. 4. UCH-L1 expression in neurogenesis. NPCs were immunolabeled with antibodies against TuJ1 and UCH-L1. Cultures were counterlabeled with Hoechst nuclear dye to facilitate cell quantification. Quantitative analysis of the percentage of cells stained with each antibody. (A) In the proliferating phase (+bFGF; at 48 hours) or the differentiation phase (–bFGF; 2, 12, 24, 48 hours), most TuJ1-positive cells co-express UCH-L1. The UCH-L1 expression level is both high and low in TuJ1-positive cells at 48 hours. (B) Quantitative analysis of the percentage of cells stained with each antibody. The number of TuJ1-positive cells gradually increased in the differentiating phase (–bFGF; B). Each experiment was analyzed by counting cells in three independent wells at the indicated times. The experiments were repeated at least two times. Bars, 50 μm.

categorized into at least two subgroups based on their UCH-L1 expression (Fig. 3A,B).

UCH-L1 and TuJ1 expression in cultured NPCs

We then analyzed the expression patterns of UCH-L1 and TuJ1. In the presence of bFGF, TuJ1-positive cells were rarely detected. However, in the absence of bFGF, TuJ1-positive cells were induced. In the cultures without bFGF, as the UCH-L1 single-positive cell population decreased with time, the UCH-L1/TuJ1 double-positive population increased (Fig. 4A,B). UCH-L1/TuJ1 double-negative cells were detected in the differentiating phases at 6, 12, 24 and 48 hours. UCH-L1/TuJ1 double-negative cells might be the nestin single-positive cells at 6 hours and 12 hours in Figs 3 and 4. TuJ1 single-positive cells were infrequently detected in the differentiating NPCs. Because 71.4±3.4% of NPCs differentiated into TuJ1-positive cells under our culture conditions without bFGF at 48 hours, almost all UCH-L1-positive cells are thought to differentiate into TuJ1-positive neuronal cells (Fig. 4A,B). The differentiating NPCs included TuJ1-positive cells in which UCH-L1 was either strongly or weakly expressed (Fig. 4A). These data indicate that UCH-L1-positive NPCs have a high potential for differentiating into neuronal cells and that TuJ1-positive neuronal cells are heterogeneous with regard to UCH-L1 expression.

Morphological classification of UCH-L1-positive NPCs

Nestin is a marker of undifferentiated cells, whereas UCH-L1 is a neuron-specific marker. Here, UCH-L1/nestin double-positive cells were present in cultured NPCs as well as in embryonic brain (Figs 2, 3). Cultured NPCs sequentially gave rise to neurons, then astrocytes, and finally oligodendrocytes (data not shown). Under our culture conditions, neurogenesis actively occurred in differentiating NPCs between 2 and 12 hours after plating (Fig. 4). Glial differentiation had not begun by this time. We collected differentiating NPCs at 6 hours and 12 hours after plating and then analyzed the morphology of nestin-positive cells (Fig. 5). Both UCH-L1/nestin double-positive cells and nestin single-positive cells were present in the population of differentiating NPCs. As the population of double-positive cells might represent a progression of differentiating neurons, we examined the morphology of these cells. Differentiating neurons undergo a stereotypical set of morphological changes, including length (from long to short) (Fukuda et al., 2003; Hartfuss et al., 2003; Nadarajah et al., 2001). We categorized the nestin-positive cells with respect to process length (long, short or round; Fig. 3). UCH-L1 single-positive and double-negative cells were included in the total number of cells. When the total length of processes was more than four times the diameter of the nucleus of the cell, the cell was categorized as 'long', whereas cells with shorter processes were categorized as 'short'. Cells that did not have processes were classified as 'round'. At 6 hours, the majority of nestin single-positive cells were long (18.2±7.6% vs 4.0±0.2% short cells; mean±s.d.; Fisher's PLSD, P=0.008), whereas the majority of UCH-L1/nestin double-positive cells were short (62.0±6.3%). This population was significantly greater than that of long cells (10.3±2.0%) and round cells (5.0±1.7%; Fisher's PLSD, P<0.0001). When NPCs with processes were subcategorized as unipolar, bipolar or multipolar, the unipolar population was significantly higher (62.3±16.9%) than the bipolar population (18.2±3.9%; Fisher's PLSD, P=0.002) in UCH-L1/nestin double-positive cells. Multipolar cells were not observed at 12 hours. However, in nestin single-positive cells, more NPCs were bipolar (16.5±4.6%) than unipolar (4.5±1.9%; Fisher's PLSD, P=0.009; Fig. 6B). Similar results were obtained at 12 hours (Fig. 6). Thus, most UCH-L1/nestin double-positive cells had shorter processes and were more likely to be unipolar.

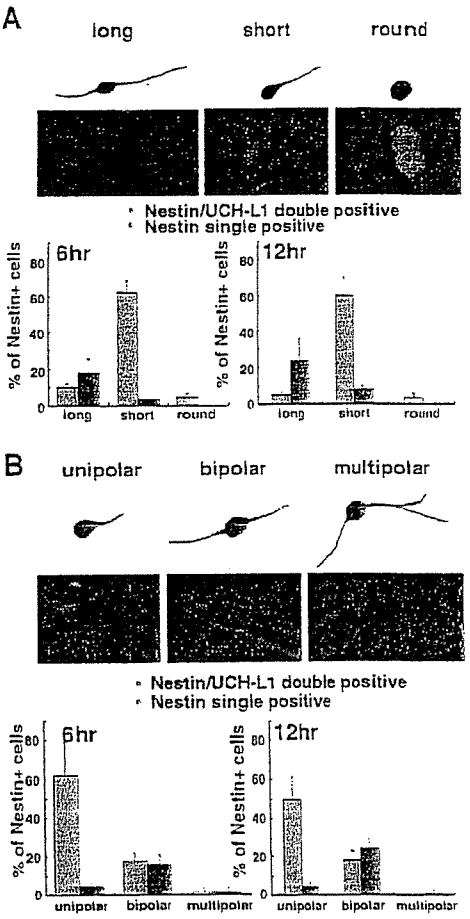

Fig. 5. Morphological identification of subpopulations of cultured NPCs at 6 and 12 hours after induction of differentiation. Differentiating NPCs were double stained with UCH-L1 and nestin. For the quantification depicted in A, differentiating NPCs stained with UCH-L1 and nestin were classified as long, short or round (see text). For the quantification depicted in B, differentiating NPCs were classified based on three kinds of cell morphology: unipolar, bipolar, or multipolar.

Effect of UCH-L1 on nestin-positive processes

We next examined the effect of UCH-L1 on proliferating NPC morphology using the transient transfection method. NPCs were allowed to proliferate for 48 hours after transfection and were then induced to differentiate for 12 hours. The cells were fixed, and the length of nestin-positive processes was examined. To quantify the relationship between UCH-L1 expression and process formation, we measured the total length